TURUN YLIOPISTO

STRUCTURAL CONTROL OF GOLD DEPOSITS IN THE HUITTINEN AREA, SW FINLAND

Kasper Koivukangas

Kallioperägeologia
Pro gradu -tutkielma
Laajuus: 30 op

Ohjaaja:
Pietari Skyttä

22.12.2022
Turku

Master's thesis

Subject: Bedrock Geology
Author: Kasper Koivukangas
Title: Structural control of gold deposits in the Huittinen area, SW Finland
Supervisor: Pietari Skyttä
Number of pages: 56 pages
Date: 12.22.2022

The purpose of this thesis is to investigate the relationship between bedrock structures and orogenic gold deposits in the Huittinen area, southwestern Finland by the means of bedrock mapping and structural analysis. The study area contains five known gold occurrences and one active orogenic gold mine at Jokisivu. The study aims at recognizing structural trends and discontinuities, which may indicate new target areas for gold exploration. Mapping and analysis of these geological features is important for understanding structures controlling the transport of ore-forming fluids and emplacement of gold bearing quartz veins. Orogenic gold deposits are usually found in subsidiary structures that splay from first-order structures. The main focus during the field work was obtaining structural information from the bedrock so that further analysis and interpretation could be made to correlate the trends and kinematics of faults and shear zones to the existing tectonic models and previous studies. Although bedrock mapping was focused on structural features, lithologies are important as well. For example, mafic rocks such as gabbros are interesting as they might act as traps for gold bearing hydrothermal fluids. The study area is bound by two major shear zones, Kynsikangas SZ in the west and Kankaanranta SZ in the south. Thus, the secondary objective was to examine their relationship with each other as intersections of major structures are considered highly potential for orogenic gold deposits. The study area was divided into northern and southern subareas based on spatial clustering of the observations. Foliation and lineation measurements revealed similar characteristics in both subareas, foliations exhibiting ~E–W and NW–SE trending sets whereas mineral lineations are steeply plunging to ~NE. Regional folding exhibits fold axes that plunge steeply towards ~NE as well. Quartz-feldspar veining is common and typically foliation-parallel throughout the study area. Pegmatites have been emplaced in at least two phases as older generation have been deformed together with the host rock whereas the younger set of pegmatites crosscut sharply other rocks and lack any mesoscopic deformation textures. Bedrock mapping with the aid of aeromagnetic anomaly map resulted in the identification of a distinct shear zone parallel to the Kankaanranta SZ in both subareas. Furthermore, a third NW–SE trending shear zone was recognized in the northern subarea. The known gold occurrences within the study area are spatially associated with these ENE–WSW and ~NW–SE trending shear zones. The nature and contrasting kinematics of structural discontinuities indicate that the observed fault and shear patterns formed in separate deformation phases. For example, brittle subsidiary structures associated with originally ductile shear zones with contrasting kinematics indicate that the older ductile shear zones reactivated under brittle or brittle-ductile regime when the crust had cooled down.

Key words: orogenic gold, Huittinen, structural geology, Svecofennian orogeny

Pro gradu -tutkielma

Pääaine: Kallioperägeologia
Tekijä: Kasper Koivukangas
Otsikko: Structural control of gold deposits in the Huittinen area, SW Finland
Ohjaaja: Pietari Skyttä
Sivumäärä: 56 sivua
Päivämäärä: 12.22.2022

Tämän Pro gradu -tutkielman tarkoitus on tarkastella kallioperän rakenteiden ja orogeenisten kultaesiintymien välistä suhdetta Huittisten alueella Lounais-Suomessa kallioperäkartoituksen ja sen pohjalta tehtävän rakenneanalyysin avulla. Tutkimusalueella on viisi tunnettua kultaesiintymää toiminnassa olevan Jokisivun kultakaivoksen lisäksi. Tutkimuksen tavoitteena on tunnistaa kallioperän rakenteiden trendit ja epäjatkuvuudet, joiden avulla voidaan paikantaa uusia kohdealueita kullan etsinnässä. Näiden geologisten piirteiden kartoitus ja analysointi on tärkeää, jotta ymmärrettäisiin malmin muodostumista kontrolloivia rakenteita, jotka ohjaavat fluidien kulkeutumista ja kultapitoisten kvartsijuonten asettumista kallioperään. Tyypillisesti orogeenisia kultaesiintymiä esiintyy toisen kertaluokan rakenteissa, jotka haarautuvat pääsiirroksesta tai -hiertovyöhykkeestä. Kenttätyön päätavoitteena oli rakennedatan kerääminen, jonka perusteella alueen rakennegeologista historiaa ja kinematiikkaa voidaan tulkita ja edelleen tarkastella sen yhteensopivuutta aikaisempiin tutkimuksiin ja olemassa oleviin tektonisiin malleihin. Myös litologiset havainnot ovat tärkeitä, sillä esimerkiksi mafiset kivet, kuten gabrot, ovat tyypillisesti isäntäkivenä tutkimusalueen kultaesiintymissä. Tutkimusaluetta rajaa kaksi hiertovyöhykettä, Kynsikankaan hiertovyöhyke lännessä ja Kankaanrannan hiertovyöhyke etelässä. Tutkimuksen toisena tavoitteena olikin tutkia niiden suhdetta toisiinsa, koska suurten rakenteiden risteyskohtien katsotaan olevan erittäin potentiaalisia orogeenisille kultaesiintymille. Tutkimusalue on jaettu eteläiseen ja pohjoiseen osa-alueeseen havaintojen alueellisen jakautumisen perusteella. Liuskeisuus- ja lineaatiomittausten perusteella molemmat osa-alueet ovat samankaltaisia. Liuskeisuus muodostaa kaksi suuntasettiä, joiden kulkusuunnat ovat itä–länsi- ja luode–kaakko -suuntaisia, kun taas alueellinen poimuakseli ja mineraalilineaatiot kaatuvat jyrkästi kohti koillista. Kvartsi-maasälpäjuonet ovat yleisiä ja usein liuskeisuuden suuntaisia. Pegmatiitteja on muodostunut ainakin kahdessa vaiheessa. Vanhemmat pegmatiitit ovat olleet mukana duktiilissa deformaatiossa, kun taas myöhemmät pegmatiitit leikkaavat terävästi muita kiviä eikä niissä havaittu deformaatiotekstuureja. Kallioperäkartoitus yhdessä aeromagneettisen anomaliakartan avulla johti Kankaanrannan hiertovyöhykkeen suuntaisten hiertovyöhykkeiden tunnistamiseen molemmilla osa-alueilla. Lisäksi pohjoisella osa-alueella tunnistettiin luode–kaakko -suuntainen hiertovyöhyke. Tutkimusalueen kultaesiintymät liittyvät alueellisesti näihin ~itä–länsi- ja luode–kaakko -suuntaisiin hiertovyöhykkeisiin. Hiertovyöhykkeiden ja niistä haarautuvien rakenteiden luoma geometria sekä kinemaattiset indikaattorit viittaavat siihen, että havaitut siirrokset ja hiertovyöhykkeet muodostuivat useassa deformaatiovaiheessa. Esimerkiksi kinematiikaltaan vastakkaiset hauraat toisen kertaluokan rakenteet, jotka haarautuvat alun perin duktiileista hiertovyöhykkeistä osoittavat, että ne uudelleenaktivoituivat, kun kuori oli jäähtynyt.

Avainsanat: orogeeninen kulta, Huittinen, rakennegeologia, Svekofenninen orogenia

Table of Contents

1 Introduction

Structural control of gold deposits has been recognized for a long time (e.g. Boyle 1961; Anhaeusser 1976; Fryer et al. 1976; Groves & Phillips 1987). In addition, Bohlke (1962) noted the spatial and temporal association of gold bearing quartz veins and orogenic belts. Furthermore, epigenetically occurring structurally hosted lode-gold deposits in metamorphic terranes have been described by Kerrich (1993). These types of deposits have been compiled into a single class of orogenic gold deposits by Groves et al. (1998).

Most gold deposits in Finland have been identified as orogenic gold deposits (Eilu 2015). The orogenic gold mineralizations in Finland are associated with Archean greenstone belts, areas between the Archean and Proterozoic domains such as Raahe-Haapajärvi and Savo districts along the Raahe-Ladoga zone, and all major supracrustal belts of southwestern Finland (Eilu et al. 2003; Eilu 2012). In addition, orogenic type gold mineralizations may have overprinted other gold deposits such as the gold rich Haveri volcanogenic massive sulphide (VMS) deposit in SW Finland (e.g. Vaasjoki & Huhma 1987; Nironen 1994), where earlier mineralization is associated with hydrothermal fluids venting on sea floor in an early-stage island arc setting (Mäkelä 1980).

The multiphase deformational processes associated with Svecofennian orogeny that took place between 1.92 and 1.77 Ga played a major role in producing gold mineralizations in SW Finland (Korsman et al. 1999; Lahtinen et al. 2005; Eilu 2012). The structural control of mineralization is evident in many of the gold deposits in SW Finland (e.g. Saalmann 2007; Saalmann et al. 2009, 2010). In addition, timing for these gold mineralizations has been constrained with mainly structural interpretations revealing that mineralization took place in the late stages of the Svecofennian orogeny between 1.82 and 1.75 Ga (Saalman 2007; Saalmann et al. 2010; Molnár et al. 2017a).

The purpose of this thesis is to investigate the relationship between bedrock structures and orogenic gold deposits in the Huittinen area, SW Finland by the means of bedrock mapping and structural analysis. The study aims at recognizing structural trends and discontinuities, which indicate new target areas for gold exploration. This said, a structural analysis and interpretation of the study area is provided as it is critical for understanding the geometry of the pathways that ore-forming fluids have moved through the crust and further caused emplacement of gold bearing veins.

Even though bedrock mapping was focused on structural features, lithologies are important as well. Especially, mafic rocks such as gabbros are interesting as they might act as traps for gold bearing hydrothermal fluids (e.g. Saalmann et al. 2010; Kara et al. 2021). Also, mafic to felsic supracrustal rocks have been spatially associated with gold occurrences in SW Finland (e.g. Saalmann 2007; Saalmann et al. 2009).

The study area is bound by two major shear zones: a roughly N–S striking Alastaro shear zone in the west (Pitkälä 2019) and an ENE–WSW trending Kankaanranta shear zone in the south (Leskelä 2019). In addition, there may be a connection between the roughly N–S trending Kynsikangas shear zone and the Kolinummi and Hämeenlinna shear zones located northwest, southwest, and south of the study area, respectively (Väisänen & Skyttä 2007; Saalmann et al. 2009; Reimers et al. 2018).

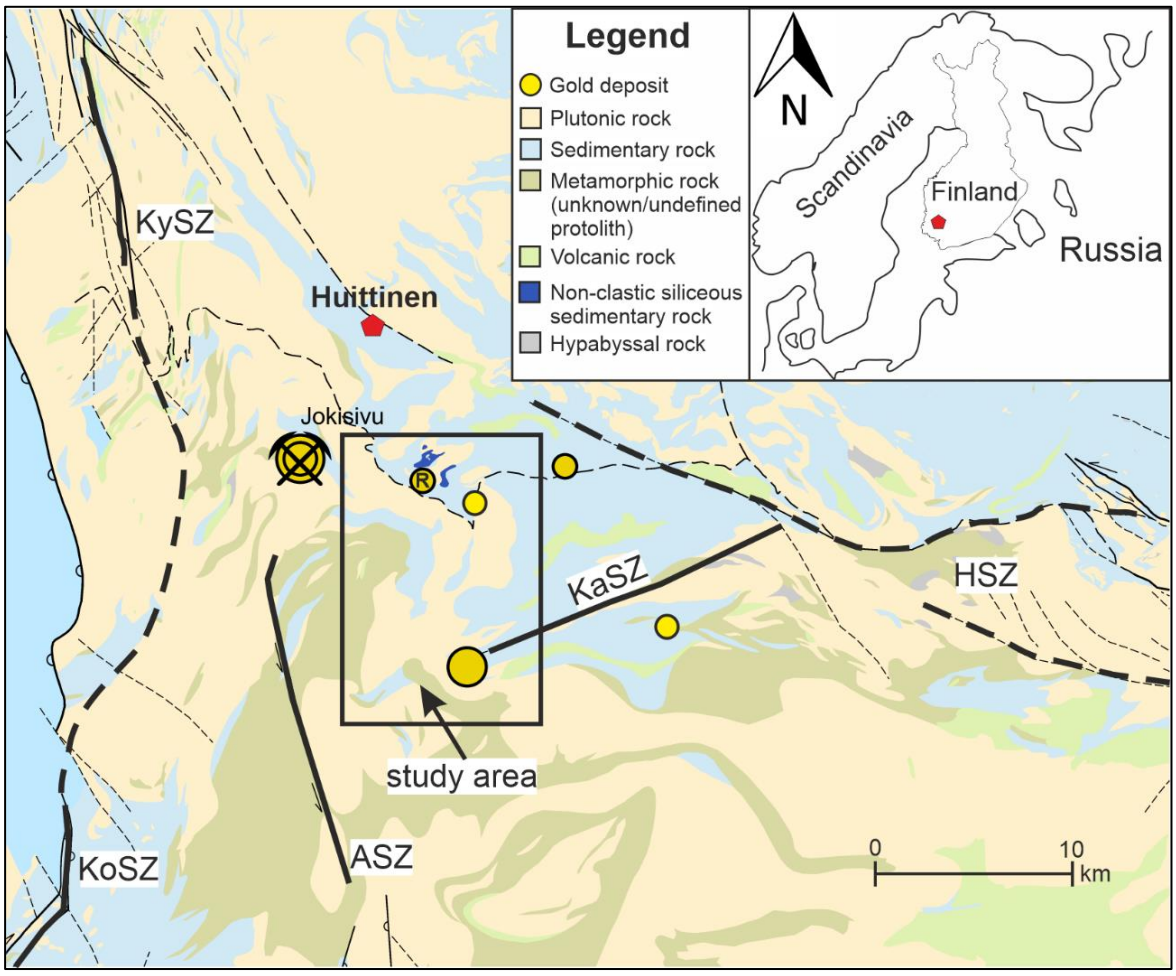

Figure 1. Major shear zones surrounding the study area and known gold occurrences including Jokisivu gold mine. ASZ = Alastaro shear zone, HSZ = Hämeenlinna shear zone, KaSZ = Kankaanranta shear zone, KoSZ = Kolinummi shear zone, KySZ = Kynsikangas shear zone, R = Ritakallio. Generalized lithological map is provided by the Geological Survey of Finland.

The Alastaro shear zone may be a linking feature between the Kynsikangas and Kolinummi shear zones. Thus, the secondary objective of this thesis was to examine the relationship between the shear zones bounding the study area. Most importantly, intersections of major

structures are considered highly potential for orogenic gold deposits (e.g. Hronsky et al. 1990; Fedorowich et al. 1991; Peters 1993a, b). Moreover, recognizing first-order structures can lead to improved understanding about the second and third order structures that commonly hosts orogenic gold deposits (Robb 2005).

The study area and its immediate surroundings contain five known gold occurrences and one active gold mine at Jokisivu (Fig. 1). The two southernmost gold occurrences are spatially associated with the KaSZ whereas the northern part of the area contains three gold occurrences and the Jokisivu gold mine (Fig. 1). The northern gold occurrences host rocks have been cut by localized structures and quartz veins controlling the localization of gold but have yet to be linked to a specific major shear zone (Luukkonen et al. 1992; Vuori et al. 2005; Grönhölm & Voipio 2012). Although, it has been proposed that the gold-hosting ~E–W trending shear zones at Jokisivu splay from regional-scale NW–SE trending structures (Saalmann et al. 2010). Also, gold critical structures in Ritakallio have similar, roughly E–W and NW–SE orientations (Vuori et al. 2005).

1.1 Definition of orogenic gold

Before the term orogenic gold was widely accepted, the literature was crowded by different classifications for gold only and lode-gold deposits in metamorphic terranes (e.g. Phillips & Powell 1993; Kerrich 1993). Thus, papers published before Groves et al. (1998) proposed the classification of orogenic gold deposits using many different terms of these type of deposits, which is why I think it's necessary to address the history and differences of the terminology used in this context.

According to Groves et al. (1998) there was an elevated interest in describing gold deposits driven by the rise of gold prices during the late 1970s, which led to a wide variety of classification terms based on different parameters along with numerous synonyms for similar types of deposits, further leading to confusing and inconsistent nomenclature as the knowledge of gold deposits accumulated rapidly (e.g. Cox & Singer 1986; Robert et al. 1991).

Groves et al. (1998) pointed out that many classification terms are geographical as they refer to type localities of a specific deposit type such as Motherlode- (e.g. Poulsen 2000) and Korean-type (Shelton et al. 1988). Also, many similar types of deposits have been classified with terms that reflect the ore-forming temperature, depth, or host rock of the deposits. For example, previously used terms such as Archean gold-only, mesothermal greenstone-gold and syn-orogenic Mother lode, each reflecting a particular spatial or temporal association, actually

represent subtypes of structurally hosted lode-gold deposits that occur epigenetically in metamorphic terranes (Kerrich 1993).

Term *mesothermal gold* gained some popularity after Nesbitt et al. (1986) described lode-gold deposits associated with accreted terranes forming at 200–350°C temperatures. According to Groves et al. (1998) using the term mesothermal in this context is not appropriate, as it should be limited to deposits with rather narrow depth range of about 1.2 to 3.6 km (Lindgren 1933). Hence, *mesothermal* is better suited for deposits in the gold porphyry and skarn environments or Carlin-type deposits (Poulsen 1996). Instead, Groves et al. (1998) proposed that the gold deposits with many common features could be lumped together into a single class of orogenic gold deposits.

This said, there wasn't a consistent classification term for gold deposits that were emplaced at near surface to mid-crustal levels, which is unique for hydrothermal ore deposits until the orogenic type of gold was described by Groves et al. (1998) as the authors recognized the need for a broader classification reflecting the widely varying depth of formation and spatiotemporal association with orogeny that epigenetic, structurally hosted lode-gold deposits in metamorphic terranes exhibit. Most importantly, recognizing common features between these deposits helped to describe and develop further this classification scheme.

Regardless of the age of these deposits, the common features included were: i) late or post-peak metamorphic mineralization, ii) back-arc or fore-arc tectonic environment, iii) extensive depth of possible ore formation, iv) introduction of carbon dioxide and water together with K, S, Si and Au by hydrothermal fluids, along with different amounts of As, B, Bi, Na, Sb, Te and W, but with low concentration of base metals, and v) chemically similar and supralithostatic ore-forming fluids (Gebre-Mariam et al. 1995; Groves et al. 1998; Goldfarb et al. 2001, 2005). Although, it must be noted that the pressure conditions fluxuate and multiple stages of gold mineralization takes place under different pressure conditions (Tavares Nassif et al. 2022).

This classification solves numerous inconsistencies within the earlier nomenclature regarding structurally controlled gold deposits associated with orogenic processes bringing them under a single class, which is why it has been firmly established in the geological literature (e.g. Groves et al. 1998; Goldfarb & Groves 2015; Groves et al. 2020). Although, it must be noted that terminology used today is still somewhat inconsistent (e.g. Phillips & Powell 2015).

1.2 The main characteristics of orogenic gold

Orogenic gold deposits, which produce roughly one-thirds of world's gold together with intrusion related gold (Frimmel 2008), have been forming globally throughout the Phanerozoic era and episodically from the Middle Archean to the younger Precambrian for more than 3 billion years (Goldfarb et al. 2001). They are closely linked to deformation processes that take place during the formation of orogens as hydrothermal fluids emplace gold bearing quartz veins along the structural discontinuities (Groves et al. 1998; Robb 2005). Furthermore, the active intervals of orogenic gold formation in Precambrian settings are associated with supercontinent cycles as these periods actively produced orogens (Goldfarb et al. 2010). This said, orogenic gold is spatially associated with major structures in the bedrock (Goldfarb et al. 2001). For example, intersections of major structures are considered highly potential for orogenic gold deposits (e.g. Hronsky et al. 1990; Fedorowich et al. 1991; Peters 1993a, b).

Albeit being spatially and temporally linked with major faults and shear zones, orogenic gold deposits rarely occur within these first-order structures (McCuaig & Kerrich 1998). There have been several hypotheses as to why this is the case. For example, Robb (2005) listed three suggestions: i) Eisenlohr et al. (1989) proposed that temperature differences between first order and subsidiary structures may favour gold deposition into the latter, ii) Kerrich (1989a, b) suggested that the ductile nature of first-order structures is the key factor, whereas iii) lower mean stress in the surrounding rocks than within the first-order structures was pointed out by Ridley (1993) and Groves et al. (1995). Most importantly, recognizing the second and third order structures is crucial as many individual deposits and mines lie within these subsidiary faults and shear zones (Robb 2005).

Timing of the orogenic gold deposits can be interpreted as both post- and syn-orogenic. For example, the post-orogenic interpretation is valid as the host rocks surrounding the ore may have already been cooling and experiencing uplift during ore formation, whereas the ore-forming fluids could be viewed as syn-orogenic, since they may have resulted from the ongoing subduction driven thermal processes at depth (Groves et al. 1998; Stuwe et al. 1993). This said, the gold mineralization typically takes place slightly after regional peak metamorphism while being subject to compression or transpression in accretionary or collisional tectonic setting in the late stages of orogenesis following a clockwise P-T-t path (McCuaig & Kerrich 1998; Goldfarb et al. 2001; Groves et al. 2003; Molnár 2017b; Ranta &

Molnár 2018). Furthermore, the deposit formation typically takes place during shifts in the stress regime from compression to transpression or transtension (Goldfarb & Groves 2015).

In these tectonic environments water-bearing sediments and volcanic rocks are accreted to the continental margin, which together with the subduction-related increasing pressure and temperature conditions leads to the migration of hydrothermal fluids (Groves et al. 1998). In addition, the deeper the fluids are, the less space they have to move within the rocks. Hence, structural features become important as deformation-driven faulting and shearing allow the opening of pathways for these fluids (e.g. Sibson & Scott 1998; Robb 2005). According to Goldfarb & Groves (2015), there are multiple possible subduction-related scenarios where devolatilization of the subducting slab may occur, leading to the release of metamorphic fluids that migrate upwards in the crust to from orogenic gold deposits. These include: i) crustal thickening, ii) plume impact/subduction, iii) subduction rollback, and iv) oceanic ridge subduction.

By dividing epigenetic or near-surface gold-rich mineral deposits with respect to their tectonic setting illustrates well how orogenic gold deposits differ from the other near-surface gold deposits as transcrustal structural discontinuities acting as pathways for hydrothermal fluids increase the depth range of possible orogenic gold mineralization (Fig. 2a). Nevertheless, the emplacement of gold in deformed and metamorphosed rocks of all ages at mid-crustal, typically 3–15 km depths is characteristic for orogenic gold deposits (Goldfarb et al. 2001; Goldfarb & Groves 2015). Terms *epizonal*, *mesozonal* and *hypozonal* are used to indicate different depths and metal associations of orogenic gold emplacement (Groves et al. 1998; Fig. 2b).

The host rocks of the mineralized gold-bearing quartz veins are variable and show some correlation with geological time as most Archean orogenic gold are hosted by greenstone dominated areas, i.e., metamorphosed volcanic rock sequences that also include subvolcanic intrusions, banded iron formations and to a lesser degree, typically clastic sedimentary rocks. By contrast, Phanerozoic deposits are commonly hosted by thick and extensive sedimentary rock sequences. In addition, intrusive granitic host rocks of all ages predating the ore deposition are known as well (Goldfarb & Groves 2015).

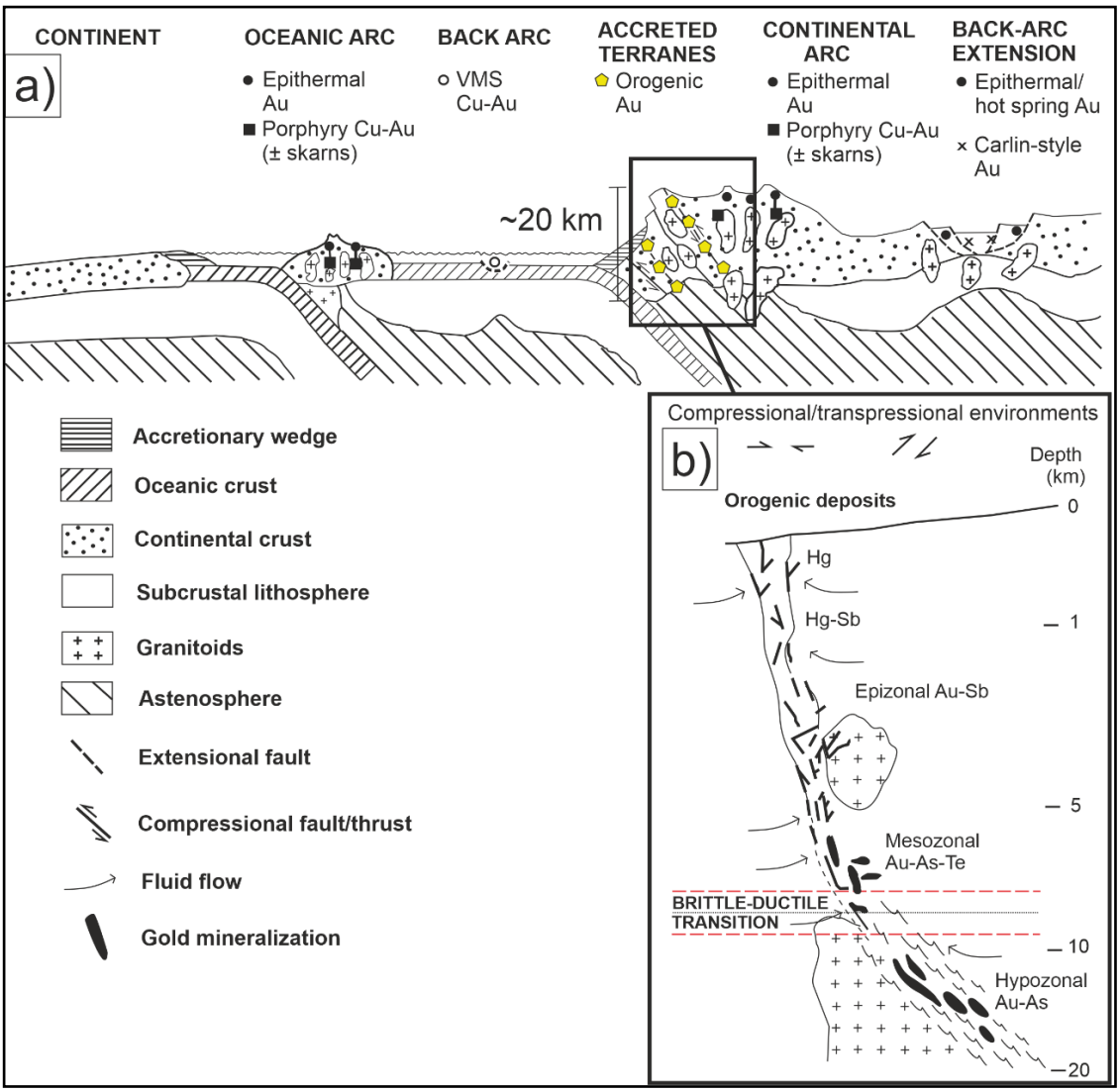

Figure 2. a) Tectonic setting of near-surface gold deposits with emphasize on the depth of orogenic gold deposits that may form at 20 km of depth. b) Epizonal deposits are formed close to the surface with less than 6 km in depth, mesozonal deposits are emplaced at 6–12 km of depth, and hypozonal deposits represent the deepest ones forming at 12–20 km of depth. Modified after Groves et al. (1998) and Goldfarb & Groves (2015).

1.3 Ore-bearing orogenic fluids

The gold is transported as a reduced sulphur complex in the ore-bearing orogenic fluids that contain water and carbon dioxide with or without methane and have almost neutral pH of 5.5 and low salinity of 3 to 7 wt.% NaCl equivalent (Groves et al. 1998; Goldfarb & Groves 2015). Elevated CO_2 concentrations of ≥ 5 mol% and δ18O values of 5 to 8 per ml in Archean greenstone belts and 7 to 9 per ml in Phanerozoic vein hosted gold are typical (Groves et al. 1998). In addition, similar δ18O values of 6 to 11 per ml were obtained by McCuaig & Kerrich (1998) for Precambrian fluids, whilst Bierlein & Crowe (2000) showed the CO_2 concentrations of the Phanerozoic fluids to be consistently between 7 and 13 per ml. Furthermore, the relatively high content of CO_2 most likely allows the fluids to have the near

neutral pH that is crucial for the reduced sulphur complex to attain high gold solubility (Phillips & Evans 2004).

Other parameters affecting the gold solubility in hydrothermal fluids are PT-conditions and the amount of ligands such as chloride and sulphur (e.g. Stefansson & Seward 2004). The host rock might have a control on which process is the primary engine for the gold precipitation from hydrothermal fluids. For example, the most important mechanism for gold precipitation in metasedimentary host rocks, that have clear evidence of hydrofracturing, is considered to be decompression, which may lead to phase separation within the fluid, and hence enhancing the gold deposition (e.g. Bowers 1991; Hayashi & Ohmoto 1991). By contrast, studies involving iron rich Precambrian rocks indicate that fluid-rock interaction is the most important gold precipitation mechanism (e.g. Groves & Phillips 1987). Especially, the sulphidisation of the wallrock seems to be the most important gold precipitation mechanism at all crustal levels (Mikucki 1998).

There are multiple models regarding the source for auriferous fluids that remain under consideration: i) magmatic-hydrothermal, ii) metamorphic crustal fluid, iii) metasedimentary and metavolcanic rock source for Phanerozoic and Precambrian orogenic gold, respectively (Goldfarb & Groves 2015). Data from fluid inclusion and stable isotope studies seem to indicate that models implying metamorphic origin for the ore fluids are more viable (Groves et al. 2020). For example, fluid inclusion studies show that these fluids are non-aqueous and rich in CO_2 indicating that meteoric water and magmatic-hydrothermal source is not possible (e.g. Kerrich 1989c). The consistency in fluid inclusion compositions rules out models that imply mixing of fluids from multiple sources in majority of the deposits. Nevertheless, the fluids can be affected by or derived from the crust (Goldfarb & Groves 2015).

1.4 Orogenic gold in Finland

The gold production didn’t have a significant role in Finland before the opening of Kittilä gold mine in 2009 (Puustinen 1991, 2003). Furthermore, the largest VMS deposits in Finland (Outokumpu, Pyhäsalmi, and Vihanti) produced most of the gold before the year 2000 (Eilu 2015). Currently there are four active gold mines in Finland: i) Kittilä mine in Lapland, ii) Laiva mine in North Ostrobothnia, iii) Pampalo mine in North Karelia, eastern Finland, and iv) Jokisivu mine in Satakunta, southwestern Finland (Fig. 3; GTK-MDAE 2022).

According to Eilu (2015) the improvement in analytical methods and understanding of the geology and gold deposit formation together with the increasing gold prices led to elevated

interest in Finnish gold deposits and exploration. This said, there are now more than 200 gold deposits and occurrences indicated by drilling in Finland with new ones discovered every year (Fig. 3).

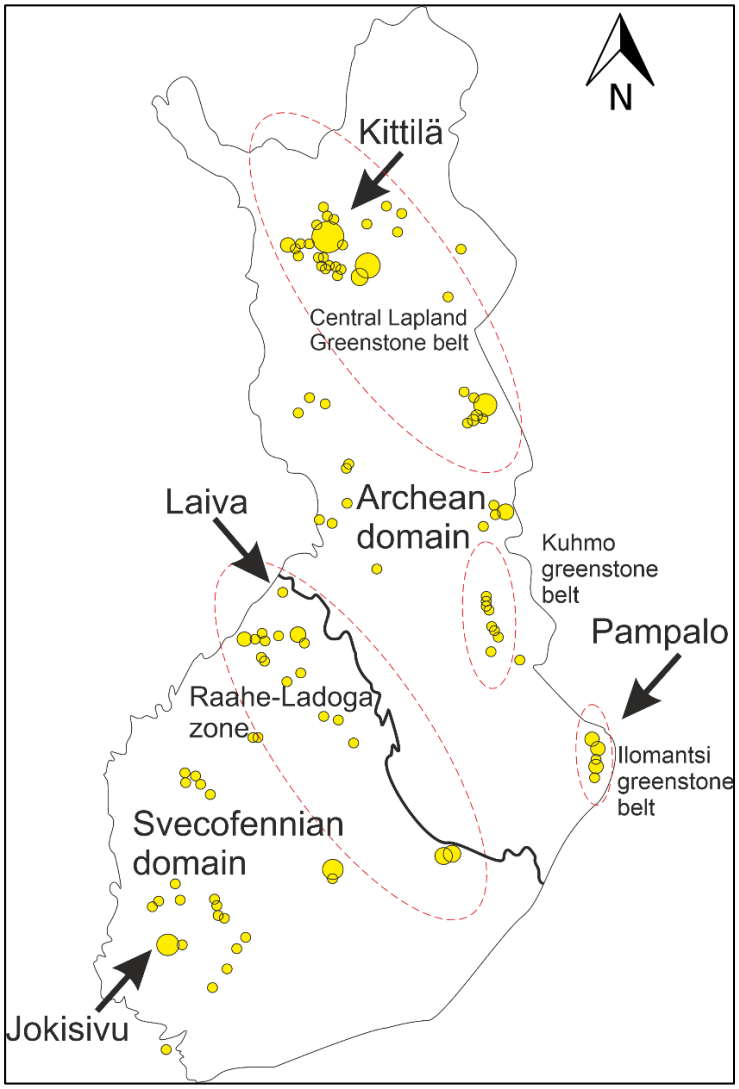

Figure 3. Simplified map showing orogenic gold deposits in Finland with Svecofennian and Archean domains, and areas associated with orogenic gold deposits. Active gold mines pointed with arrows. Modified after GTK (2020).

The orogenic gold mineralization events in Finland are associated with Archean greenstone belts, areas between the Archean and Proterozoic domains such as Raahe-Haapajärvi and Savo districts along the Raahe-Ladoga zone, and all major supracrustal belts of southwestern Finland (Fig. 3; Eilu et al. 2003; Eilu 2012). According to Eilu (2015) approximately 90 % of the gold deposits in Finland are of the orogenic type. The formation of these deposits has taken place episodically in the late Archean between 2.75 and 2.70 Ga and Paleoproterozoic between or slightly after 1.89 and 1.86 Ga (Eilu et al. 2003) continuing until ~1.75 Ga (Molnár et al. 2017a).

The Proterozoic rocks have a significant importance as they host the majority of the orogenic gold occurrences in Finland (Eilu et al. 2003; Sundblad 2003). Generally, sedimentary and mafic host rocks are common (Eilu et al. 2003), but intermediate to felsic igneous and sedimentary host rocks are more typical in the Svecofennian domain (e.g. Korsman et al. 1997; Eilu 2012). The gold mineralization (and alteration) occurs in rocks that have undergone metamorphism in upper greenschist to lower amphibolite facies (Eilu et al. 2003).

Southwestern Finland contains many gold deposits of different types such as orogenic gold, gold rich VMS, epithermal gold, and granitoid-related gold (Eilu 2012). Orogenic gold deposits can be found in all supracrustal belts of SW Finland, although their relative proportion is different in each belt. For example, all gold occurrences in Pohjanmaa and Pirkanmaa Belts are considered to be orogenic, whereas orogenic type gold seems to be a minority in the Uusimaa Belt, which is dominated by VMS and epithermal type gold (Eilu 2012 and references therein). In addition, orogenic gold deposits are the most abundant type as it covers about 60 % of all gold occurrences in SW Finland (Eilu & Pankka 2010).

The characteristics of orogenic gold deposits in SW Finland indicate that they were formed during the late stages of the Svecofennian orogeny at 1.82–1.78 Ga (Saalmann 2007; Saalmann et al. 2010). Furthermore, gold mineralization in the Svecofennian domain has taken place under amphibolite facies P-T conditions (Eilu et al. 2003).

2 Geological context

2.1 Tectonic evolution of Fennoscandia

The bedrock of Finland is part of the Fennoscandian Shield that consists dominantly of Precambrian rocks of the Fennoscandian crustal segment that is part of the East European Craton (Gorbatschev & Bogdanova 1993). The East European Craton comprises of Fennoscandia, Volgo-Uralia, and Sarmatia crustal segments bound by the Caledonides in the northwest, Timanian fold belt in the northeast, and Trans-European Suture Zone in the southwest (Fig. 4).

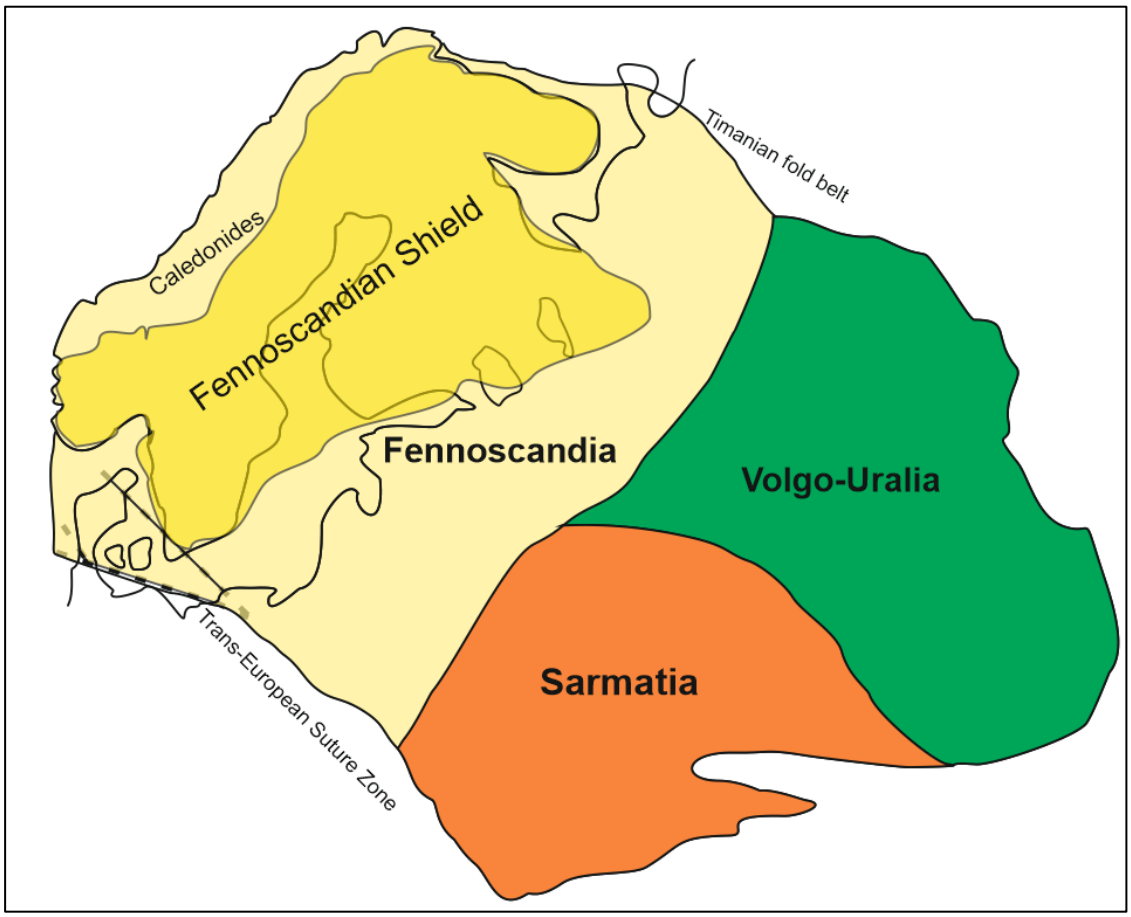

Figure 4. The Fennoscandian Shield and crustal segments of the Eastern European Craton. Modified after Gorbatschev & Bogdanova (1993).

The Fennoscandian Shield has a long and complex tectonic history (e.g. Lahtinen et al. 2005; Nironen 2017). It comprises of five tectonic provinces (Karelia, Lapland-Kola, Norrbotten, Sveconorwegia, Svecofennia) that by definition have been separated from each other by an ocean before amalgamation. Therefore, they share common tectonic history only after these lithospheric blocks merged with each other to form the Fennoscandian protocontinent (Nironen 2017). Four of the Fennoscandian Provinces form the bulk of the Precambrian

bedrock in Finland (Fig. 5). The final assembly of these four lithospheric blocks took place during the Svecofennian orogeny between 1.92 and 1.86 Ga (Nironen 2017).

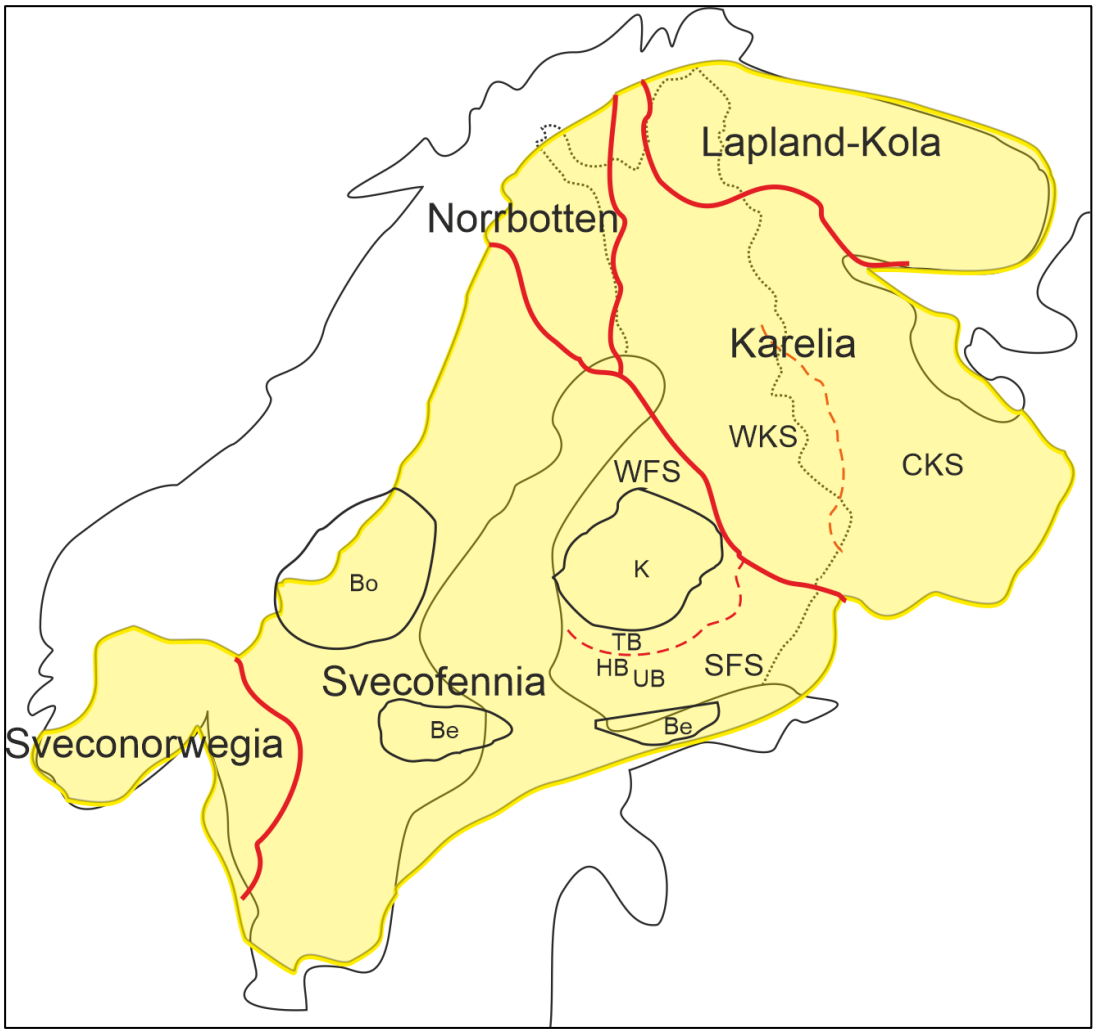

Figure 5. Tectonic provinces of the Fennoscandian Shield (yellow area). Be = Bergslagen microcontinent, Bo = Bothnian microcontinent, CKS = Central Karelian Subprovince, HB = Häme Belt, K = Keitele microcontinent, SFS = Southern Finland Subprovince, TB = Tampere Belt, UB = Uusimaa Belt, WFS = Western Finland Subprovince, WKS = Western Karelian Subprovince. Modified after Korja et al. (2006) and Nironen (2017).

The Karelia, Lapland-Kola, and Norrbotten provinces comprise of both Archean and Proterozoic rocks (Nironen 2017). The Archean basement of Karelia province formed during 3.1–2.68 Ga and involved accretion of exotic terranes of subsequent collisional crustal stacking, and eventually, formation of a new Neoarchean continent, the Karelian craton (Hölttä et al. 2012). Also, the Archean rocks in Lapland-Kola province were initially part of the Karelian craton but extensional events taking place at 2.68–2.1 Ga separated the Archean blocks of Lapland-Kola and Karelia from each other and an ocean formed in between (Daly et al. 2001; Nironen 2017). Later a shift from extensional regime to contractional one started to bring these lithospheric blocks back together initially through accretion that started at 1.95 Ga (Daly et al. 2006).

This accretionary stage ended around 1.92 Ga, which also marks the beginning of the main collisional stage of the Svecofennian orogeny as the amalgamation of Fennoscandian shield initiated (Nironen 2017). For example, the Kola and Norrbotten cratons started to approach the Karelia craton (Korja et al. 2006). Currently the Norrbotten and Karelia provinces are separated by Pajala shear zone (Lahtinen et al. 2015). Also, prior to the collision with the Karelia craton, the Norrbotten craton had a volcanic arc accreted to it (Lahtinen et al. 2005). In contrast to the aforementioned provinces, the Svecofennia province consists almost only of Proterozoic rocks, and it has been divided into Western and Southern Finland subprovinces (Fig. 4; Nironen 2017), which correspond to the accretionary arc complexes of southern and central Finland as previously defined by Korsman et al. (1997).

During 1.82–1.80 Ga the Fennoscandian protocontinent collided with Volgo-Sarmatia and formed the continent of Baltica, which is represented by the East European Craton (Fig. 4; Gorbatschev & Bogdanova 1993; Bogdanova et al. 2015). Fennoscandian part of this continent kept growing by accretion for some time before stabilizing around 1.76–1.65 Ga (Nironen 2017). Afterwards Baltica experienced intracontinental rifting and magmatism in its interior parts between 1.65 and 1.1 Ga (e.g. Rämö & Haapala 2005), whereas the southwestern margin of the continent encountered several orogenic events: i) the Gothian event between 1.66 and 1.52 Ga (Åhäll & Connelly 2008), ii) the Telemarkian event at 1.52–1.48 Ga (Bingen et al. 2008), and iii) the Hallandian-Danopolian orogeny at 1.47–1.42 Ga (Bogdanova 2008). Emplacement of the rapakivi granites and related anorthosites and mafic dikes associated with the crustal rifting events were the last major additions to the Precambrian bedrock in Finland (Nironen 2017).

2.2 Evolution of the Svecofennian orogeny

Various tectonic models along with refined versions of them have been suggested for the evolution of Svecofennian orogeny over the years, and these models can be grouped into two main groups (e.g. Bogdanova et al. 2015; Nironen 2017). One group of models implies that the Svecofennian orogeny took place in a single active continental margin setting (e.g. Bogdanova et al. 2015 and references therein) whereas the other group of models infers that the evolution of the Svecofennian orogeny did not take place in a semi-continuous process but rather it comprised of several orogenic events that include four main stages represented by: i) accretion of microcontinents at 1.92–1.87 Ga, ii) extension at 1.86–1.84 Ga, iii) continental collision at 1.84–1.79 Ga, and iv) orogenic collapse and subsequent stabilization at 1.79–1.77 Ga (Lahtinen et al. 2005, 2009).

According to the latter interpretation the Svecofennian orogeny took place between 1.92 and 1.77 Ga evolving through the four major stages that partly overlap in space and time as different parts of the plate were subject to different processes (Korsman et al. 1999; Lahtinen et al. 2005; Korja et al. 2006). Furthermore, the composite Svecofennian orogen (Lahtinen et al. 2005; Korja et al. 2006) was preceded by Lapland-Kola orogeny and its main collision event between 1.94 and 1.92 Ga (Daly et al. 2006), which are considered as the two major stages of orogenic evolution in Fennoscandia (Lahtinen et al. 2009). The Lapland-Kola orogeny continued until ~1.86 Ga, hence partly overlapping with Svecofennian orogeny (Daly et al. 2006). Lahtinen et al. (2005, 2009) suggested that the Svecofennian orogeny comprises of four partly simultaneous orogenic events: the linear Lapland-Savo, Nordic, and Svecobaltic orogenies, and the equidimensional Fennian orogeny, all of which have their own tectonic histories.

The composite Svecofennian orogeny was initiated when the first major stage of accretionary tectonics took place and the Lapland-Savo orogeny (main collision at 1.92–1.91 Ga) commenced when the Norrbotten craton and Keitele microcontinent, characterized by juvenile crust, amalgamated with the Karelian craton at its western margin (Fig. 5; Korja et al. 2006). The Lapland-Savo orogeny can be divided into northern and southern segments, which formed during the collision of Karelia craton with the Norrbotten craton in the north and the Keitele microcontinent in the south, respectively (Lahtinen 2009, 2005). The Keitele microcontinent is represented by the Central Finland Granitoid Complex and is associated with an island arc complex that formed the Savo Belt along the suture zone between the Archean and Proterozoic domains during this collision event (Lahtinen et al. 2005, 2009). The Norrbotten craton in the north is represented by the Kittilä allochton (Lahtinen et al. 2005).

Subsequently, the Bothnian microcontinent collided to the continental collage continuing its westward growth and changing the plate motions leading to subduction switchover as northern subduction was locked under the southern margin of Keitele microcontinent, which is represented by the Tampere Belt (Fig. 5; Korja et al. 2006). By contrast, the southern subduction initiated moving under the Bergslagen microcontinent and the combined Häme island arc, which are represented by the Häme and Uusimaa Belts, and the Bergslagen area (Fig. 5; Korja et al. 2006). The closure of an ocean south of Keitele ended the southern subduction as the Bergslagen microcontinent collided with Keitele, which marks the beginning of the Fennian orogeny (Korja et al. 2006). The main collision stage of the Fennian orogeny took place at 1.89–1.86 Ga, which included accretion of Paleoproterozoic arcs and the Bergslagen microcontinent, which is in contrast to the earlier collisional events that were

characterized by continent-continent type collisions (Lahtinen et al. 2005, 2009). During the Fennian orogeny the volcanic belts (Häme, Tampere, and Uusimaa) in between the accreted Bergslagen and Keitele microcontinents underwent significant shortening (Korja et al. 2006).

After the Fennian orogeny, an extensional stage followed in Fennoscandia at 1.86–1.84 Ga, later followed by two continental collisions that finalized the Svecofennian orogeny (Lahtinen et al. 2005; Korja et al. 2006). First, the transpressional Svecobaltic orogeny (1.83–1.79 Ga) was initiated by the collision of Fennoscandia and Sarmatia in the SE (Lahtinen et al. 2005, 2009). The Svecobaltic orogeny was accompanied with the almost synchronous Nordic orogen (~1.82–1.79 Ga), which was probably related to the collision between Fennoscandia and Amazonia that took place in the central and northern parts of the western margin of Fennoscandia (Lahtinen et al. 2005, 2009). The magmatic and tectono-metamorphic events that took place during the Svecobaltic and Nordic orogenies between 1.84–1.79 Ga are collectively referred to as late Svecofennian (e.g. Hubbard & Branigan 1987; Ehlers et al. 1993; Jurvanen et al 2005; Väisänen & Skyttä 2007). Almost immediate orogenic collapse took place after these collisional events and the Fennoscandian Shield started to stabilize at 1.79–1.77 Ga (Lahtinen et al. 2005).

In contrast to the model described above, the other group of models explain the alternating contraction and extension phases by a migrating subduction hinge in a single active margin (e.g. Hermansson et al. 2008; Bogdanova et al. 2015). In this model the relative plate movement between the overriding plate and the subduction hinge determines whether the back-arc region of the subduction system is in contractional or extensional state (Hermansson et al. 2008). For example, subduction hinge retreating from the subduction zone infers that the back-arc region experiences extension, whereas hinge advance leads to contractional setting in the back-arc region (Hermansson et al. 2008).

Despite the two different tectonic models suggested for the evolution of Svecofennian orogeny, it is now widely accepted that it evolved through accretionary processes involving microcontinents and island arcs associated with oceanic environment linked to a rifting stage that preceded the amalgamation of Lapland-Kola and Norrbotten cratons with the Karelian craton during the onset of main collisional stage of the Svecofennian orogeny at 1.92 Ga (Korja et al. 2006; Bogdanova et al. 2015; Nironen 2017). Furthermore, multiple evidences of pre-1.92 Ga ocean or oceans exists in Fennoscandia. For example, magmatism with oceanic affinity in the 2.02 Ga Kittilä allochton (Hanski & Huhma 2005), island arc magmatism

between 1.98 and 1.96 Ga in the Kola region (Daly et al. 2006), and the 1.95 Ga Jormua ophiolite complex (Peltonen & Kontinen 2004).

2.3 Häme and Pirkanmaa Belts

The study area lies in the border zone of the western parts of the Häme and Pirkanmaa Belts, which are separated by a suture (Lahtinen 1994, 1996) that marks the boundary between the Western Finland and Southern Finland subprovinces (Fig. 6; Nironen 2017). Furthermore, the Tampere and Pirkanmaa Belts, and the Central Finland Granitoid Complex north of these belong to the Central Svecofennian Arc Complex, whereas the Häme and Uusimaa Belts are part of the Southern Svecofennian Arc Complex (Korsman et al. 1997).

The Pirkanmaa Belt is situated between the Tampere and Häme volcanic Belts (Fig. 6). It is characterized by turbiditic greywackes that formed on ocean floor (Lahtinen et al. 2009) and were later migmatized ca. 1.88 Ga forming tonalitic and trondhjemitic leucosomes (Kilpeläinen 1998; Mouri et al. 1999). These migmatized greywackes and schists were intruded by gabbros and granodiorites around 1.89–1.88 Ga (Korsman et al. 1999). The Pirkanmaa Belt is abundant in orogenic gold deposits, in fact all gold deposits in the belt are most likely orogenic in origin (Eilu 2012).

The Häme Belt is situated between the Pirkanmaa and Uusimaa Belts (Fig. 6). It consists dominantly of volcanic rocks that can occasionally be observed with alternating layers of greywackes and pelites, also plutonic rocks are common as well. The Häme Belt has been affected by strong overprinting during the late Svecofennian (1.84–1.79 Ga) orogenic events, which is characteristic for Southern Finland Subprovince (Saalmann et al. 2010).

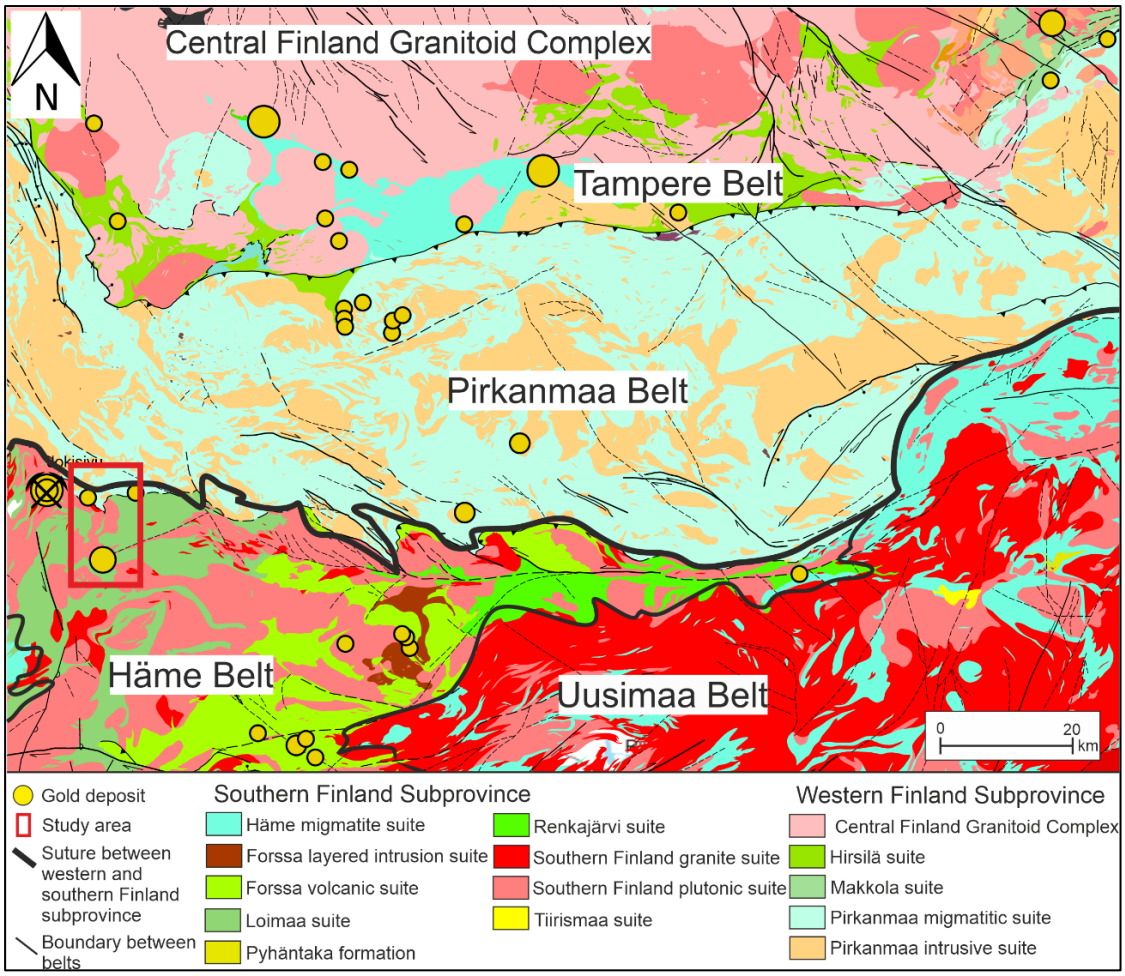

Figure 6. The Häme, Tampere and Pirkanmaa Belts and southernmost part of Central Finland Granitoid Complex on a generalized geological map by Geological Survey of Finland (GTK-MDAE 2022).

According to Tianen et al. (2017), the Häme Belt contains multiple gold deposits with total ore reserves estimated at 170 tonnes, of which 70 tonnes is orogenic gold, and it has been estimated that more than 80 % of the orogenic gold reserves are still undiscovered as only 11 tonnes have been classified as known ore reserves. Furthermore, the Häme Belt is known to host other deposits as well, such as base metal (Zn, Cu, Ni), iron-titanium and lithium occurrences (Tiainen et al. 2017).

The Häme, Tampere, Pirkanmaa, and Uusimaa Belts form a E–W trending set of volcano-sedimentary sequences that were intruded by later granitoids (e.g. Korja et al. 2006 and references therein). The dominant structures within the Häme belt are the ~E–W and ~N–S trending major shear zones and associated minor NW–SE trending shear zones splaying from the major ones (Fig. 6; Väisänen & Skyttä 2007). The Tampere and Pirkanmaa Belts are characterized by E–W trending tight or isoclinal folds and axial plane schistosity in lower grade supracrustal rocks (Nironen 1989; Kilpeläinen 1998). These older structures commonly

control the orientation of shear zones that developed later in SW Finland (e.g. Nordbäck et al 2022; Väisänen & Skyttä 2007).

2.4 Host rock lithology and structural control of gold deposits in the region

The study area is located south of the Huittinen town and is approximately 6 km wide (E–W) and 13 km long (N–S) area. To date six gold occurrences are known within or nearby the study area (e.g. Luukkonen 1994; Vuori et al. 2005; Eilu 2012; Kärkkäinen et al. 2016). Most importantly, the westernmost occurrence at Jokisivu has proven to be economically viable as it has been actively mined. Other known gold occurrences are the Ritakallio, Uunimäki, Palokallio, Korvenmaa and Kanteenmaa prospects (Fig. 7).

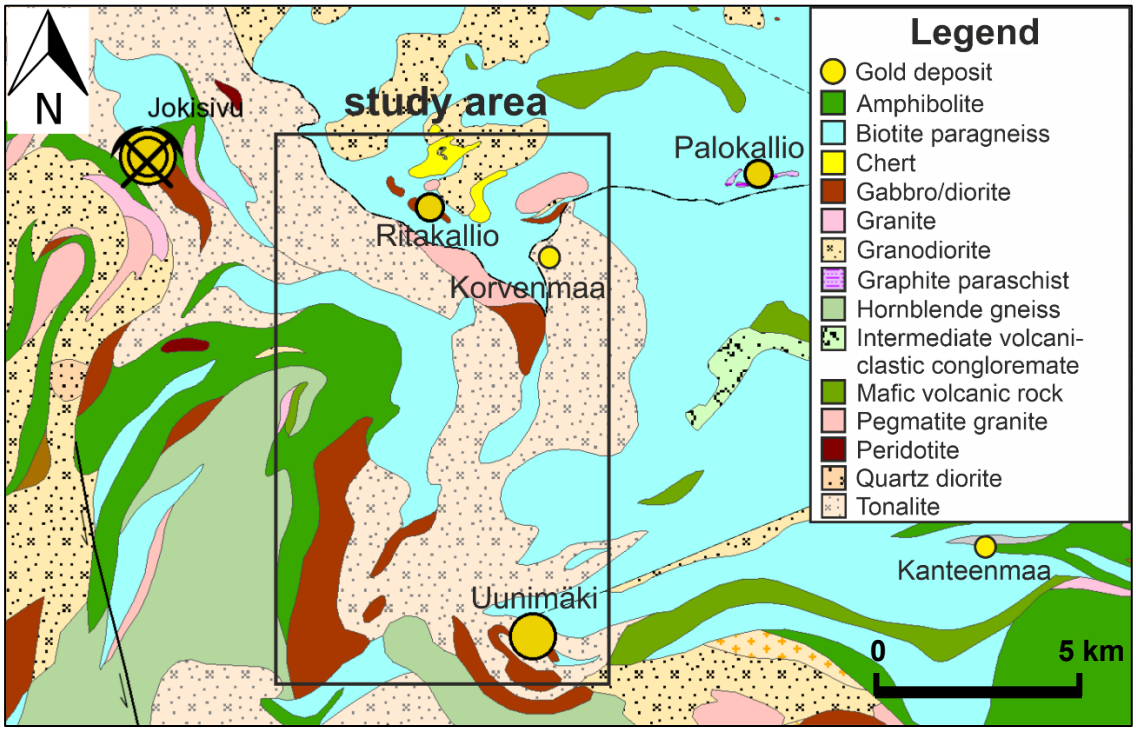

Figure 7. Study area and known gold occurrences in the region with lithological map by Geological Survey of Finland.

Host rocks in these occurrences has been described as gabbros or diorites (e.g. Eilu 2012, and references therein). However, the host rock in Uunimäki is significantly more mafic than the other intrusive host rocks in the area, and it has been suggested to be a less fractionated version of the other similar intrusions in the area based on results from geochemical analysis (Leskelä 2019; Kara et al. 2021).

The gold deposits in the Huittinen area are associated with shear zones and quartz veining indicating that their origin is within the orogenic processes. The host rocks in at least four occurrences have been cut by shear zones that control the localization of gold: i) Jokisivu dioritic intrusion has been cut by narrow shear zones that hosts fine-grained diorite, sulphides,

folded quartz veins and skarns as a result of reworking of the host material and the introduction of hydrothermal fluids (Luukkonen et al. 1992), ii) dioritic host rock in Palokallio gold occurrence is cut by narrow arsenic and sulphide bearing quartz veins associated with shear zones (Grönholm & Voipio 2012), iii) seemingly unaltered gabbro hosting the Uunimäki gold mineralization is characterized by fracture networking associated with (or splaying from) shear zones that control the localization of the gold (Kara et al. 2021), iv) gold in Ritakallio prospect is associated with shear bands and quartz veins cutting through gabbro and extending to mica gneiss (Vuori et al. 2005). In addition, the Korvenmaa and Kanteenmaa gold occurrences have not been studied yet in detail as they are merely indications from indirect exploration methods such as till geochemical data (Kärkkäinen 2007; Kärkkäinen et al. 2012).

The hosting gabbro of the Uunimäki gold occurrence has been dated by the means of zircon U-Pb geochronology revealing an age of 1891 ± 5 Ma, which is older than most similar intrusive bodies in SW Finland (Kara et al. 2021). According to Saalmann et al. (2010) the gold mineralization at Jokisivu has taken place between 1.82 and 1.78 Ga indicated by the ore hosting structures that are younger than regional fold structures, and the shear fabrics associated with gold mineralization have been correlated with late Svecofennian shear tectonics. Also, dating of the younger unaltered barren host rock, mineralized host rock, and younger pegmatite crosscutting the mineralized zone constrains the gold mineralization at Jokisivu between 1884 and 1791 Ma (Saalmann et al. 2010).

No age determination studies have been done at Ritakallio, but the gold critical WNW–ESE, ENE–WSW, and NNW–SSE trending structures (Vuori et al. 2005) are similar to the ones at Jokisivu deposit indicating that they likely formed under similar stress field and thus, represent the same age of formation. In contrast to the Jokisivu and Ritakallio occurrences, the gold in Palokallio is associated with dominantly NE–SW trending shear zones, but many other characteristics such as the mafic intrusive host rocks, ore mineralogy, and low magnetic anomaly are common between all these occurrences (Grönholm & Voipio 2012).

3 Methods

3.1 Background material

Greyscale aeromagnetic anomaly and lithological maps produced by the Geological Survey of Finland were used as background material in planning the field mapping campaigns. Preliminary field work plan consisted of two profiles each traversing across different lithological units in a N–S (profile I) and W–E (profile II) direction to get an overview of the geology in the study area (Fig. 8).

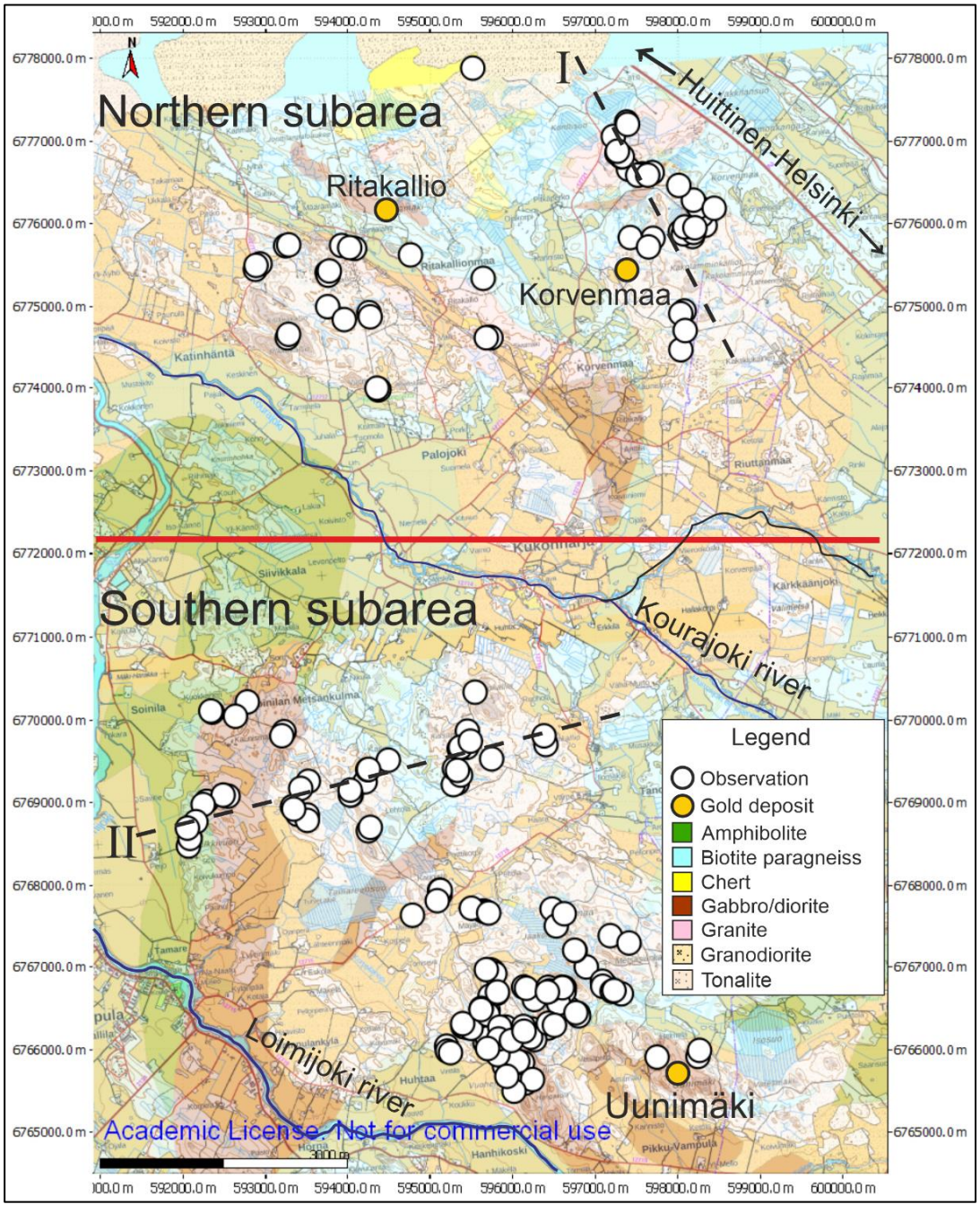

Figure 8. Localities examined in the study area and subareas divided by the Kourajoki river. Dashed lines I and II represent preliminary planned profiles to be mapped. Topographical and geological map

provided by National Land Survey of Finland and Geological Survey of Finland, respectively. Coordinates are in ETRS-TM35FIN format.

Based on earlier studies and indications of a shear zone in geophysical map, two additional areas were targeted, i) area S of Ritakallio and ii) area NW of Uunimäki (Figs. 8 & 9). The idea was to obtain field evidence of a suggested NW–SE trending shear zone near Ritakallio (Vuori et al. 2005) and of subsidiary structures in both areas, which could lead to improved understanding of how the major N–S and E–W trending shear zones are linked together.

The aeromagnetic anomaly map was very useful in identifying major faults and shear zones and was also used in structural interpretation to complement field observations (Fig. 9). For example, shear zones can be identified from aeromagnetic data due to their capability to act as pathways for fluids that often are associated with magnetite destructive alteration leading to negative magnetic anomaly along a given shear zone (e.g. Holden et al. 2012).

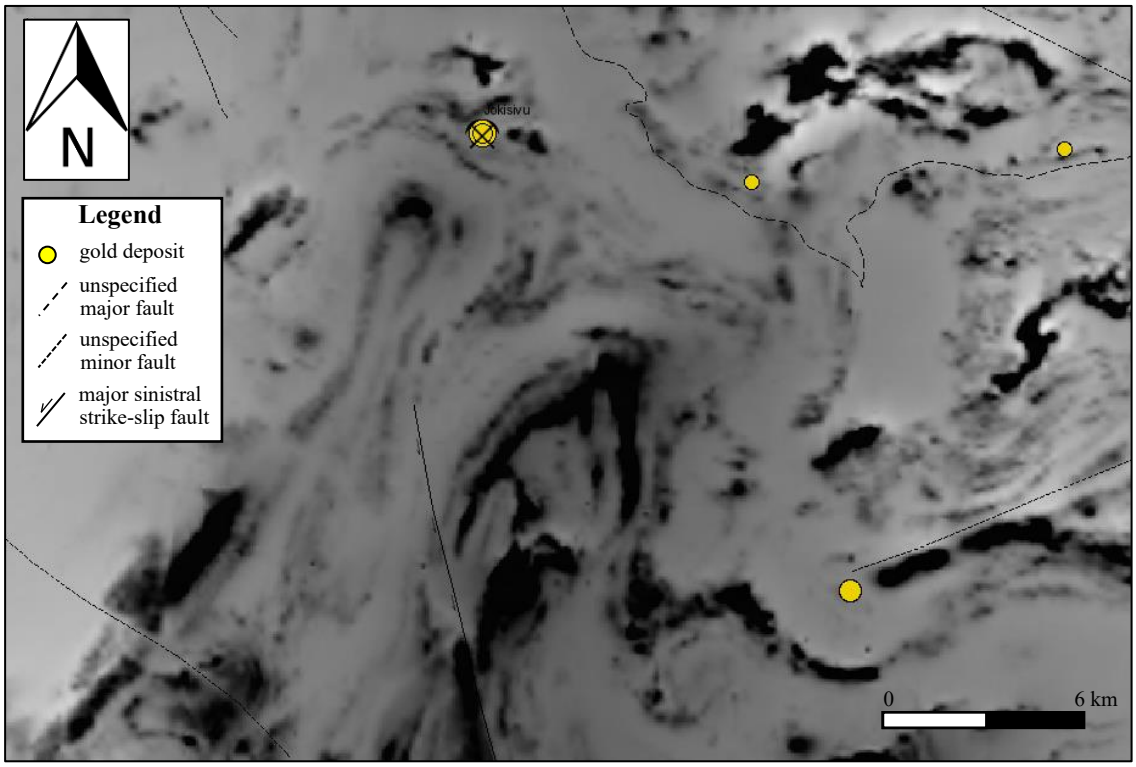

Figure 9. Aeromagnetic anomaly map, gold deposits and fault structures (shear zones) by Geological Survey of Finland (GTK-MDAE 2022).

Rock cliffs or ledges marked on standard topographical map were of great interest as these may be indicative of a fault or shear zone that was eroded more readily due to weakened mechanical strength. Furthermore, multiple ice ages have probably transported the material from the core-domains of large-scale shear zones away leaving these rock cliffs and ledges behind.

3.2 Field work

New data was collected by the means of bedrock mapping that included lithological observations, structural measurements, photos, and sketches. The main focus of the field work was to obtain structural information from the bedrock so that further analysis and interpretation, including correlation of trends and kinematics of faults and shear zones to the existing tectonic models and previous studies. During the field work a rock hammer and occasionally a chisel was used to acquire samples out from the outcrops. A hoe was used to peel off the moss on outcrops to reveal the rocks underneath, and occasionally a brush was used to clean sand and other loose material from the outcrop surfaces.

Field data was acquired from 187 localities in which one or more outcrop per locality were examined (Fig. 8). The classification of rocks is based on observations made in the field. Based on the spatial clustering of the observations the study area was divided into northern and southern subareas. The region between the subareas has very few outcrops as the roughly NW–SE trending Kourajoki river with agricultural fields on each side of it runs across the study area. Most of the studied outcrops are in forest areas that generally have decent roads due to foresting and hunting activities. Furthermore, outcrops are generally within a reasonable walking distance from roads and well accessible throughout the study area.

In total 473 structural measurements including planar features such as foliation, shear bands, veins, faults, and joints, and linear features such as mineral lineation and fold axes were taken in the field with Freiberg geological compass. No declination correction was conducted when collecting the data but +9° was later incorporated when plotting the measurements on maps and stereograms. Lithology, notes, sketches, photos, and the structural data was logged on Fieldmove application from PETEX running on Apple Ipad. Subsequent structural interpretation and analysis of the field data was carried out with MOVE™ program and its in-built stereonet tool running on PC.

4 Results

4.1 Lithology

Lithology in the study area consists dominantly of plutonic rocks such as granodiorites and gabbros, but amphibolites and mica gneisses are common as well (Fig. 10). On rare occasions metasedimentary and volcanic rocks were observed. The field observations correspond well with the lithological map with few exceptions. For example, felsic volcanic rocks were not expected but observed near the lithological contact between granodiorite and gabbro in the southern subarea (Figs. 10 & 19d). In addition, pegmatite granites were common in the study area.

The plutonic rocks consist mainly of medium-grained granodiorites that sometimes exhibit slight variation in composition towards more granitic and tonalitic versions. Also, few observations were made of slightly finer and coarser-grained versions of these granitoids (Figs. 11a, c). In addition, a slightly darker version of the granodiorite was occasionally observed in the southern subarea, which I refer to as quartz diorites (Fig. 11b). The quartz diorites were observed to a lesser extent and only in the southern subarea (Figs. 10 & 11b). They exhibit slightly darker matrix than granodiorites and commonly contain quartz-feldspar veins, whereas the granodiorites observed in this study generally exhibit less veining than the quartz diorites. Otherwise, the rock texture is similar between quartz diorites and the more common granodiorites.

The westernmost observations in the southern subarea are mainly fine to medium-grained amphibolites that are relatively strongly migmatized as granitic leucosomes may take up to half of the outcrop (Figs. 11g, h). Mica gneisses are commonly fine-grained, banded, and migmatized (Fig. 11f), and occasionally contain calc-silicate concretions. Gabbroic intrusions occur in the western side of the southern subarea as well as in the Uunimäki area and are commonly medium-grained with equigranular texture (Fig. 11e).

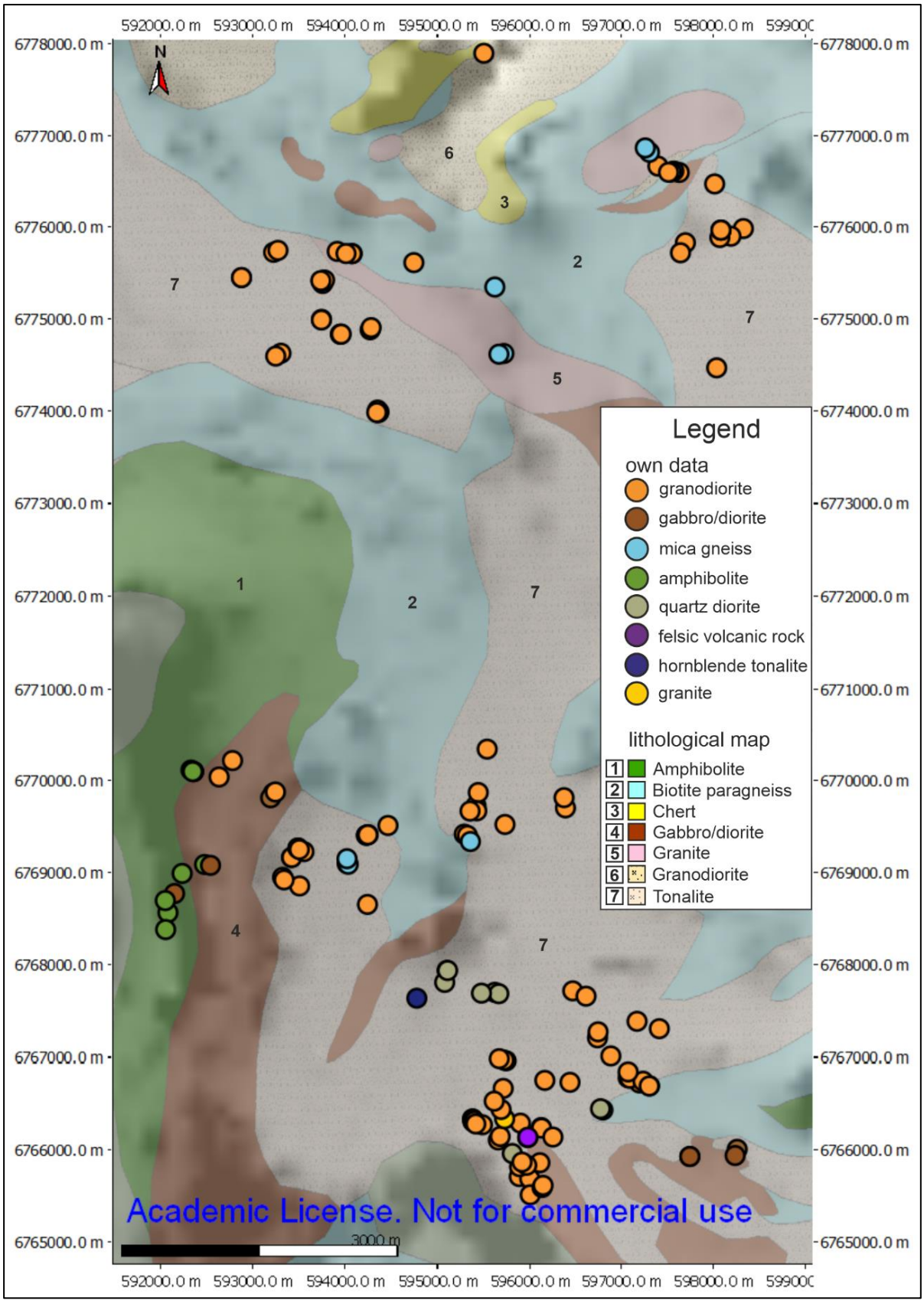

Figure 10. Lithological observations within the study area. Lithological and aeromagnetic background maps acquired from Geological Survey of Finland's webservices. Coordinates are in ETRS-TM35FIN format.

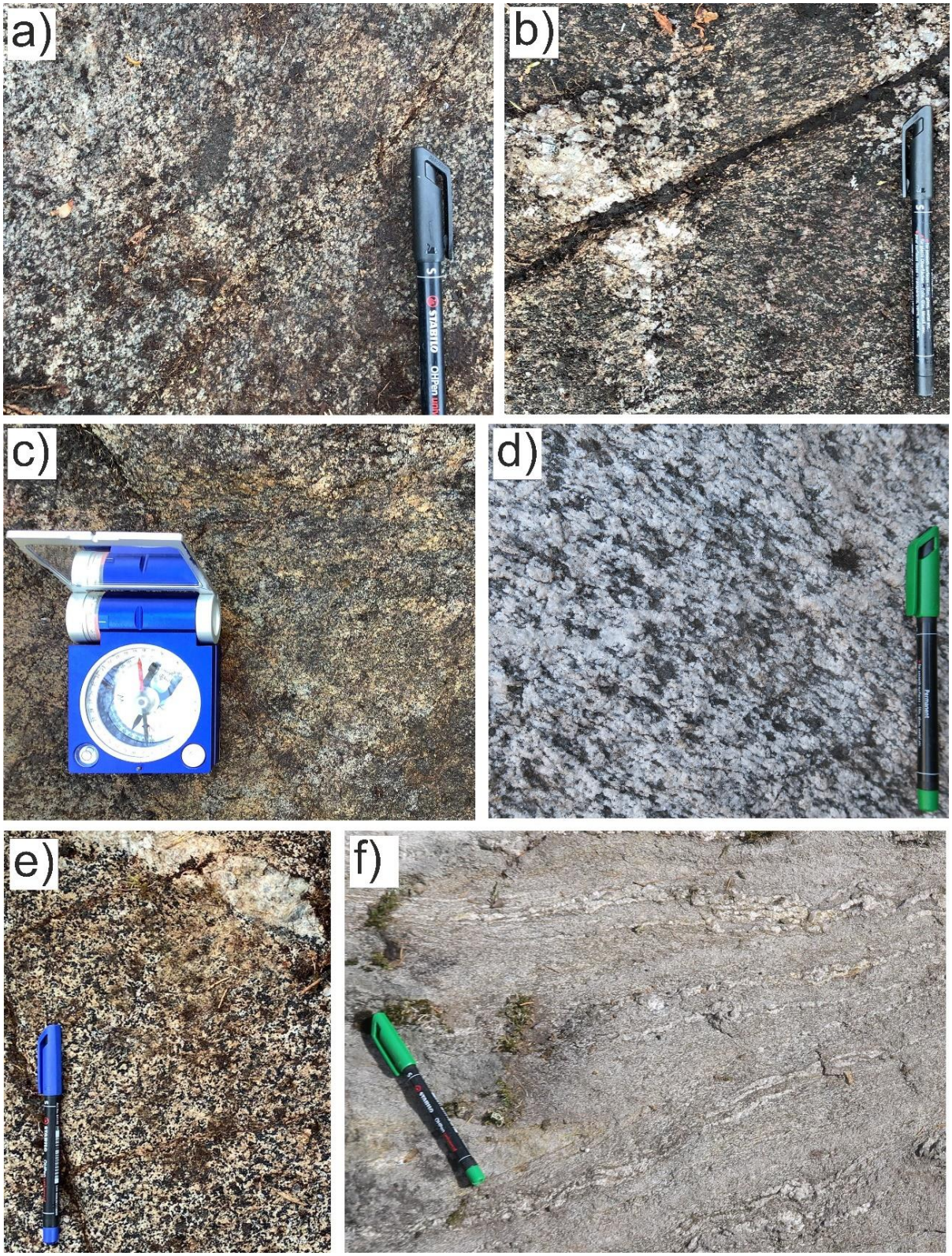

Figure 11. Caption overleaf.

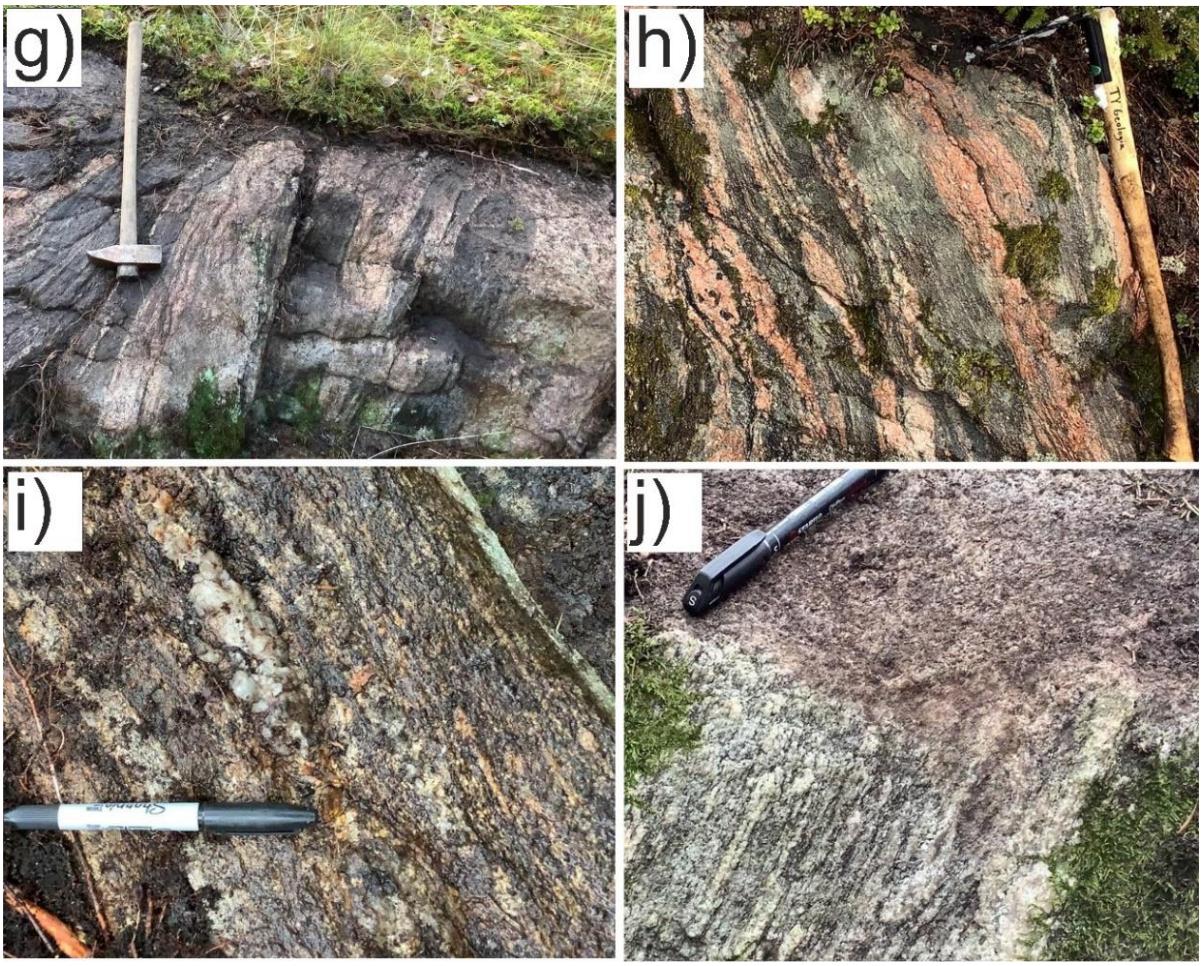

Figure 11. Most common rocks observed in the study area. a) Medium-grained granodiorite, locality 51. b) Medium-grained quartz diorite, locality 63. c) Fine-grained granodiorite, locality 42. d) Coarse-grained granodiorite, locality 152. e) Medium-grained gabbro, locality 9. f) Fine-grained mica gneiss with thin layering and leucosomes, locality 166. g) Fine to medium-grained folded amphibolite, locality 183. h) Banded amphibolite exhibiting east block up sense-of-shear, locality 8, looking to N. i) Strongly deformed granodiorite with foliation transposed to the orientation of an adjacent shear zone, locality 122. j) Granodiorite with strong lineation, locality 53. Scales: Hammer ~70 cm, pen ~15cm, compass ~8 cm.

4.2 Deformation fabrics

The most prominent feature of the granitoids observed in this study is very strong lineation and variably developed, typically weak to non-existent planar features, which are characteristic for LS- and L-tectonites, respectively. Especially, in the southern subarea this was evident as observed texture in the granitoids varied based on the angle of view. For example, a granodiorite appeared totally undeformed and equigranular on an outcrop face occurring at right angle to the mineral lineation, whereas even a slight angle in the observed face reveals the true deformation fabric of the rock (Fig. 11j). These granitoid rocks typically exhibit similar colour and texture, thus, indicating that they are probably part of the same intrusive unit.

Deformation textures in outcrop scale show amphibolites and mica gneisses exhibiting folded and banded appearance (Figs. 11f–h). Amphibolite at locality 8 shows east side up kinematics under ductile regime (Fig. 11h). The granitoids exhibit some variation in the degree of deformation fabric within the study area. This is demonstrated by the fact that weakly deformed rocks are observed in central parts of igneous bodies (Fig. 11a), whereas strongly foliated rocks are found in the vicinity of shear zones (Fig. 11i). In extreme cases the foliation is transposed into the orientation of adjacent shear zone (Fig. 15b). All in all, the strain variation is not significant excluding the high strain zones.

4.2.1 Shear zones in the northern subarea – SZ-I and SZ-III

The shear zones in this study were preliminarily identified from aeromagnetic anomaly map (Figs. 9 & 17e). There is little evidence for the SZ-I from the field, but localized deformation was recognized at locality 138 (Fig. 12b). Consequently, semi brittle felsic vein with dextral stepping and ductile buckling of the step indicates dextral kinematics at locality 174 (Fig. 12a).

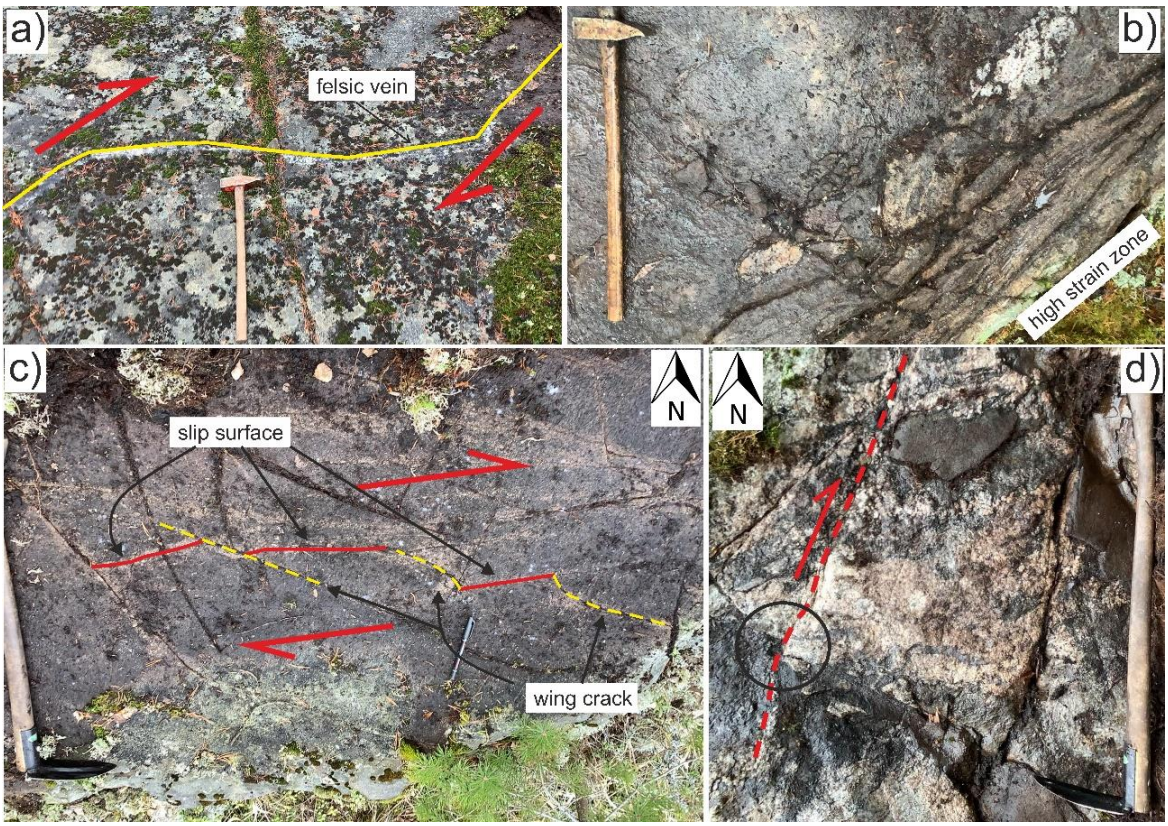

Figure 12. Structures associated with the SZ-I. a) Felsic vein exhibiting dextral stepping and semi ductile buckling of the step, locality 174, b) high strain zone in mica gneiss, locality 138, c) roughly E–W trending brittle fault with dextral kinematics indicated by wing cracking, locality 97, d) a granite crosscut by NNE–SSW trending brittle fault with ~2 cm displacement on the surface of a vertical outcrop highlighted by black circle, locality 87. Scales: pen ~10 cm, hammer/hoe ~70 cm. Hammerhead points to N.

Brittle structures associated with SZ-I exhibit dextral kinematics. For example, dextral wing cracking was observed at locality 97 (Fig. 12c). Furthermore, I have interpreted the wing cracked fault as a subsidiary Riedel shear structure splaying from SZ-I, which would also indicate dextral kinematics. Moreover, SZ-I can be traced to the west aligning with the axial plane of a large regional fold, which are known to be weakness zones in the bedrock providing more evidence for SZ-I (Fig. 17a). Also, a NNE–SSW trending dextral fault is spatially associated with the SZ-III (Fig. 12d).

The NW–SE trending dextral SZ-III is spatially close to the Ritakallio gold occurrence (Fig. 17a). On top of the "footprint" in geophysical map (Fig. 17e), tentative evidence of this shear zone was found at locality 155, where a narrow fault with alteration/deformation halo exhibits dextral kinematics implied by Riedel type shear fractures (Fig. 13b). Also, a felsic vein crosscuts sharply a weakly foliated granodiorite and a smaller felsic dike at locality 156 (Fig. 13a). The smaller felsic dike seems to have moved in a sinistral fashion, and it appears that the felsic vein has intruded into an older ductile structural discontinuity as the orientation of the smaller felsic dike is deflecting to the felsic vein indicating dextral kinematics under ductile regime and apparently sinistral kinematics thereafter (Fig. 13a).

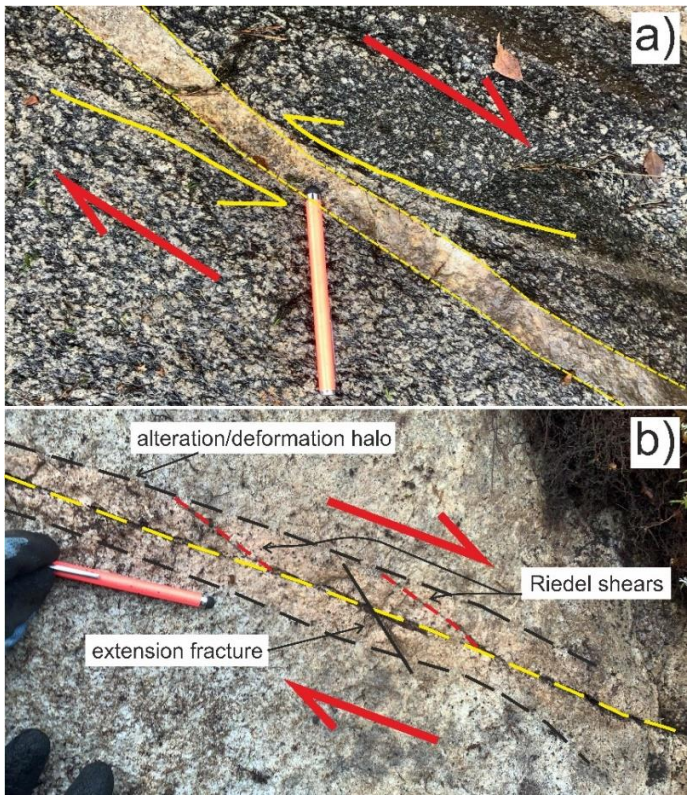

Figure 13. Structures associated with the SZ-III. a) Felsic vein crosscutting weakly foliated granodiorite and a felsic dike that exhibits sinistral displacement and marker deflection in a dextral fashion, locality 156, looking to S, b) narrow fault with deformation/alteration halo and dextral kinematics indicated by Riedel shearing geometries, locality 155, looking to S. Scale: pen ~10 cm.

The interpretation of SZ-III is based on two outcrops, localities 155 and 156 (Fig. 13). The crosscutting felsic vein and associated reverse dragged smaller felsic dike at locality 156 indicate either an earlier ductile shear zone with dextral kinematics and subsequent shift to sinistral regime or the geometry is caused by vein rotation leading to perturbation of earlier foliation (Hudleston 1989) or in this case earlier dike under continuous deformation with dextral kinematics (Fig. 13a), which correlates well with previous studies as according to Vuori et al. (2005) the gold mineralization at Ritakallio is associated with dextral shear zones.

The interpretation in the first case requires two temporally different events, ductile shear zone with dextral kinematics indicated by deflection of the smaller felsic dike and subsequent kinematic reversal under brittle regime indicated by displacement of the dike and sharp boundaries between the crosscutting felsic vein and surrounding granodiorite (Fig. 13a). Kinematic reversal has indeed been described in other studies from SW Finland as well (e.g. Nordbäck et al. 2022; Ojala 2003; Väisänen & Skyttä 2007). But there seems to be no evidence of foliation deflection in the granodiorite, only in the felsic dike. Although this may just be a matter of scale and visibility, in other words the dike is bigger and more apparent than the planar deformation fabric in the intrusive rock, and thus structural deflection is more evident in the dike.

Nevertheless, locality 155 nearby exhibits clearly dextral kinematics under brittle regime. Hence, I'm inclined to interpret the geometry at locality 156 is a result by a single continuous event where vein is formed and subsequently passively deformed (Hudleston 1989) leading to reverse drag folding (e.g. Grasemann et al. 2005). In this scenario brittle fault or crack is formed and intruded by felsic vein while being continuously deformed under the same stress field leading to vein rotation and perturbation of the smaller felsic dike, which results in sinistral reverse drag of the felsic dike under overall dextral zone (Fig. 13a).

The difference in the deformation nature of these spatially close two structures (at localities 155 & 156) could be explained by differing lithology and structure size. For example, the more ductile deformation at locality 156 might be a consequence of temporarily elevated temperature due to the heat conducting from the infill material. In contrast, due to lack of infill material in the narrow fault no additional heat from infill material is introduced and therefore, no ductile deformation is observed at locality 155. Moreover, the narrow fault exhibits alteration halo indicating the presence of hydrothermal fluids meaning that it is not a recent cracking as surface temperatures are not high enough (Fig. 13b).

4.2.2 Shear zones in the southern subarea – SZ-II

The roughly ENE–WSW trending SZ-II is almost parallel to the KaSZ and exhibits both dextral and sinistral kinematics. Evidence of sinistral brittle kinematics were observed at locality 12, where a narrow fault with roughly 5 cm left-handed displacement crosscuts two felsic dikes (Fig. 15c). By contrast, localities 13 & 122 along SZ-II exhibit dextral kinematics deforming under more ductile environment (Figs. 15a, b, d). In addition, a ~10 cm wide ultramylonitic shear zone parallel to the KaSZ with dextral kinematics indicated by S–C structures was observed at locality 146 (Fig. 14), which is located between the SZ-II and KaSZ (Fig. 17a).

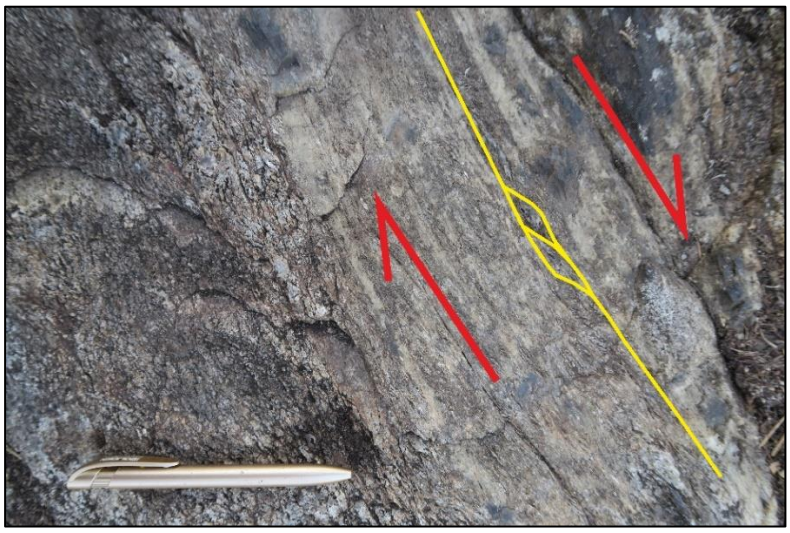

Figure 14. Ultramylonite parallel to the KaSZ exhibiting dextral kinematics indicated by S–C structures highlighted with yellow lines, locality 146. Pen (~15 cm in length) points to N.

The most prominent evidence of ductile deformation can be found in the vicinity of the interpreted SZ-II at locality 122, where drag folding along shear bands occurs, which is probably associated with the adjacent SZ-II indicate dextral kinematics (Fig. 15d). Furthermore, the rocks are highly strained close to the cliffside where they were found at, and the cliff was fractured along the foliation. Both features are typically indicative of a shear zone. In addition, SZ-II shows up in the aeromagnetic anomaly map (Fig. 17e). Also, deformation intensity is progressively weaker further away from the cliff.

The ductile deformation at locality 122 associated with SZ-II expresses open folding, shear banding, and possibly foliation boudinage structures (FBSs; Arslan et al. 2008) that might be tricky to interpret. However, interpreting the shear bands as late linking Riedel shearing (P-shear) and coupled with the folding pattern it is possible to infer a dextral sense-of-shear (Fig. 15d).

Structures apparently splaying from SZ-II include a roughly NW–SE trending shear zone that was observed at localities 36 and 38 (Figs. 15e, f). Locality 36 is characterized by anastomosing ductile shear bands with dextral kinematics indicated by foliation deflection and right-handed displacement of quartz veins (Fig. 15e). Locality 38 showcases a granodiorite that is cut by a narrow brittle fault or shear band with apparent sinistral kinematics representing later reactivation and kinematic reversal (Fig. 15f). However, the vertical component may have been more dominant in this case. A brittle ENE–WSW trending sinistral fault apparently splaying from SZ-II (Fig. 17a) was observed at locality 17 (Fig. 15g), which could be interpreted as a Riedel shear fracture, and a left-handed displacement observed at locality 12 (Fig. 15c) indicate both sinistral kinematics taking place under brittle regime.

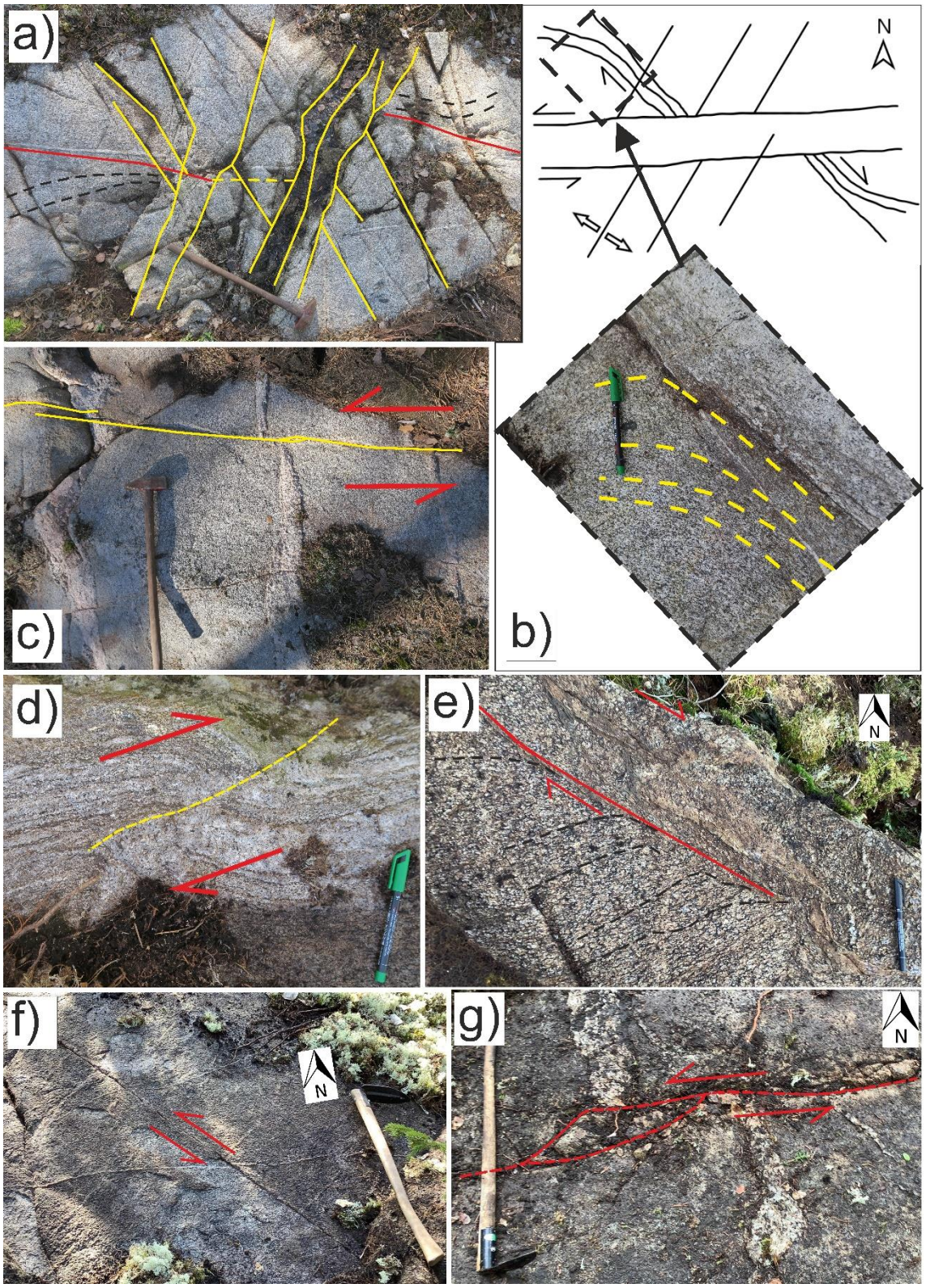

Figure 15. Structures associated with the SZ-II. a) ~E-W trending brittle sinistral fault indicated by wing cracking crosscutting a ~NW-SE trending ductile dextral shear zone indicated by foliation deflection, locality 13, b) digitized field sketch of the same outcrop and close-up photo of the foliation deflection, c) narrow brittle fault with sinistral kinematics indicated by displacement of two N–S trending felsic dikes, locality 12, d) shear band crosscutting folded and strongly foliated granodiorite with dextral kinematics indicated by drag folding along the shear band, which is associated with the adjacent SZ-II, locality 122, e) ~NW–SE trending ductile braided shearing with dextral kinematics, locality 36, f) apparently sinistral and more brittle structure in the same orientation. locality 38, g) ENE–WSW trending sinistral brittle fault crosscutting granodiorite and displacing felsic dike while exhibiting

extensional duplexing, locality 17. Pen or hammerhead points to N unless otherwise stated. Scales: hammer ~70 cm, pen ~15 cm.

4.2.3 N–S trending structures

The study area contains N–S trending structures in both subareas. These occur throughout the study area in a narrow N–S trending window roughly in the middle of the study area and include field observations such as a minor local N–S striking detachment plane cutting through a folded mica gneiss that exhibits stromatic migmatites (Figs. 16c, d), granitic mylonite exhibiting sinistral kinematics with N-S trending foliation (097/71) and mineral lineation plunging towards S (187/33) (Figs. 16a, b), hornblende rich tonalite with N–S striking foliation that is anomalous to the orientation of the immediate surroundings (Fig. 16g), ~N–S trending contact between granodiorite and mica gneiss fragment within a large intrusive unit (Fig. 16h), roughly E–W trending foliation deflecting towards N (Fig. 16e), and a N–S oriented pseudotachylite within granodiorite (Fig. 16f).

Roughly NE–SW trending dextral shear bands crosscutting gneissic banding in Z-symmetric folded mica gneiss with stromatic migmatization were observed at locality 167 (Figs. 16c, d). Furthermore, similarly a NE–SW trending dextral fault with 2 cm displacement was observed crosscutting a granite at locality 87 (Fig. 12d), roughly 1.5 km to NE from locality 167. The rheological differences in the host rock lithologies might explain the differences in the deformation style.

This said, the contrasting ductile kinematics observed at locality 167 where Z-symmetry folding and shear bands indicate dextral sense-of-shear and at locality 58 where granitic mylonite exhibit sinistral kinematics indicated by sigma clasts, may be linked to the regional folding along with SZ-I. Also, foliation deflection at locality 23 towards ~N (Fig. 16e) indicating a roughly N–S trending sinistral shear zone that could be linked to the regional folding and competence differences between lithological units (Fig. 20). The Z-symmetry folding at locality 167 corresponds well with regional folding as it spatially is associated with the northern limb of the regional fold and therefore, might represent parasitic folding (Figs. 20, 16c, d).

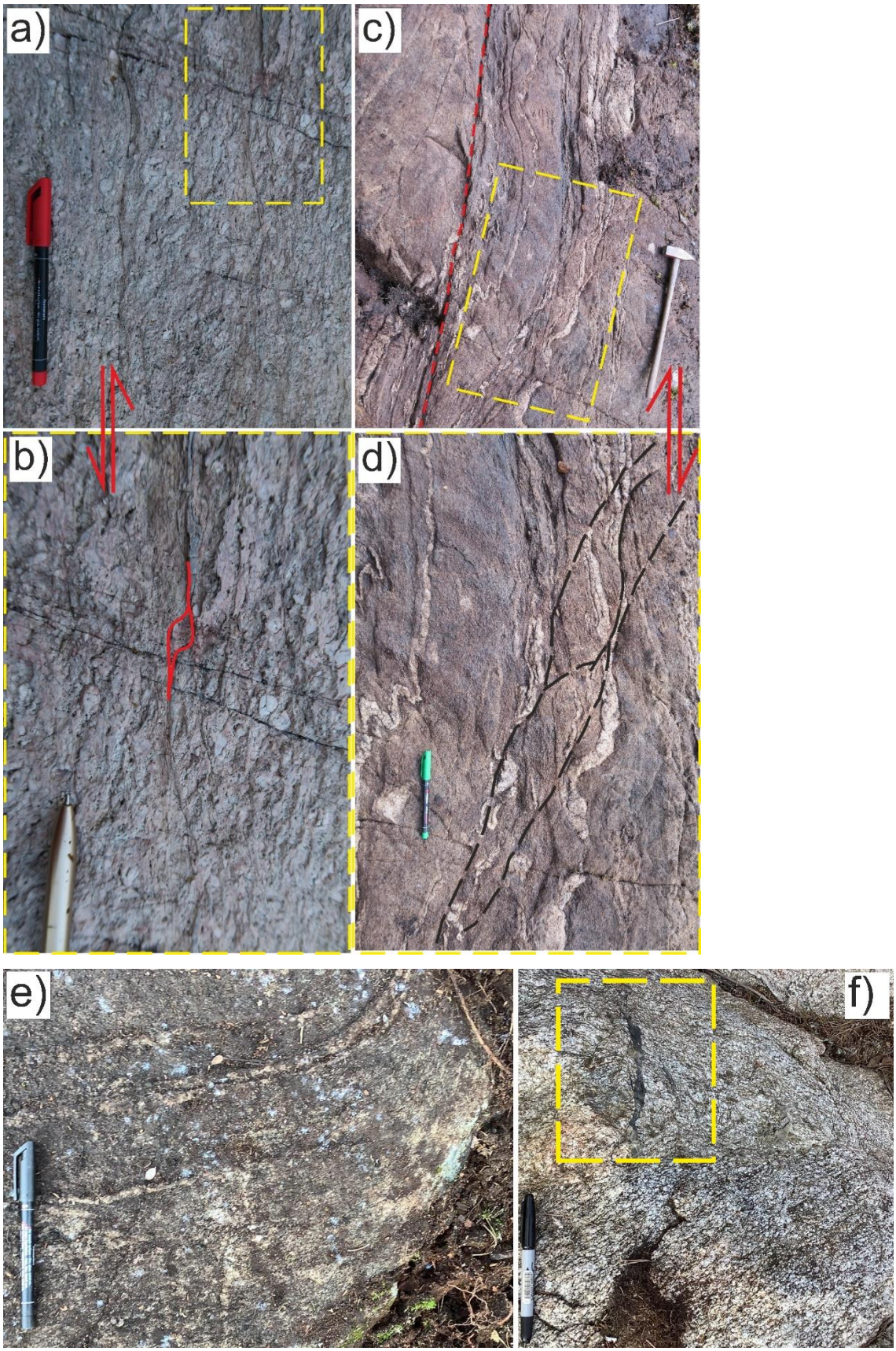

Figure 16. Caption overleaf.

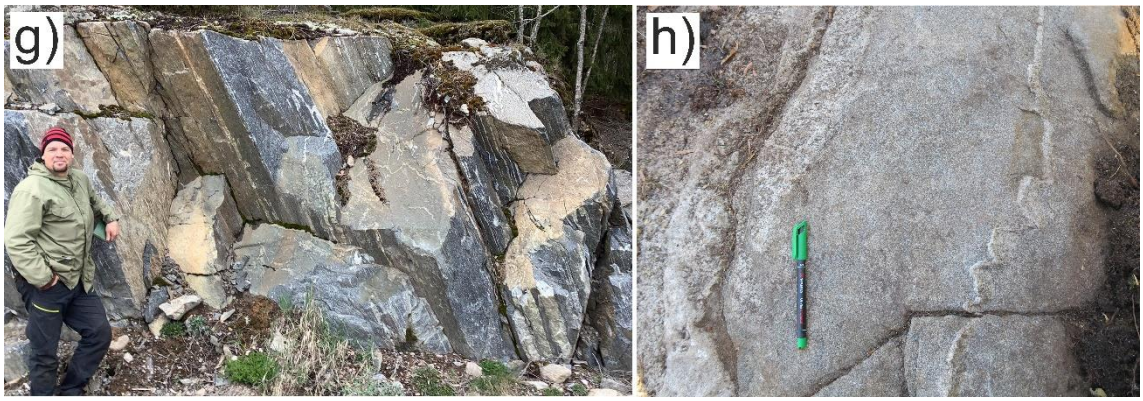

Figure 16. N–S trending structures. a) Granitic mylonite with N–S trending foliation, locality 58), b) close-up view of sigma clast indicating sinistral kinematics, locality 58, c) dextral shear bands crosscutting stromatic mica gneiss exhibiting z-symmetric folding, red dashed line highlights the N–S trending detachment plane, locality 167, d) close-up view of the dextral shear bands, e) foliation deflection towards ~N indicating a roughly N–S trending shear zone, locality 23, f) a N–S oriented pseudotachylite at locality 32 highlighted in the picture, location is almost straight towards N from the mylonite at locality 58, g) hornblende-tonalite exhibiting N–S trending foliation, view to N, locality 35, h) N–S trending contact between granodiorite and mica gneiss, locality 149.

4.3 Structural synthesis

The structural data obtained from the field is quite systematic throughout the study area. Foliation measurements can be grouped into three main sets: i) NNE–SSW, ii) ~NW–SE, and iii) ENE–WSW trending sets (Figs. 17b, c). The NNE–SSW and roughly NW–SE trending foliations are dominant in the northern subarea whereas the ENE–WSW trending foliations are dominant in the southern subarea. Mineral lineations are steeply plunging towards ~NE in both subareas (Figs. 17b, c). A total of seven fold axes were measured from five localities that resulted in mean-principal-azimuth value of 050/48 that is somewhat compatible with statistically derived fold axis (that is also known as the β-axis) value of 066/64, which indicates regional folding with steep roughly NE plunging fold axes (Fig. 17d).

The study area is cut by three roughly ENE–WSW trending structural discontinuities preliminarily identified from aeromagnetic geophysical map (Fig. 17e), and the previously studied KaSZ in the south (e.g. Kara et al. 2021). Sub-parallel or parallel to the KaSZ are the interpreted shear zones: SZ-I and SZ-II that were recognized in high strain rocks as well as from the geophysical map. A third interpreted shear zone is the NW–SE trending SZ-III that has limited field evidence but is recognizable in the geophysical map (Fig. 17e). Furthermore, multiple NNE–SSW trending shear bands were identified from outcrop observations in the northern subarea. Also, NNW–SSE trending shear bands are common in the western parts of southern subarea (Fig. 17a), which are probably related to the ductile deformation related to the regional folding (Fig. 20a).

The northern subarea contains two of the three interpreted major shear zones: SZ-I and SZ-III, along with NNE–SSW trending shear bands (Fig. 17a). The southern subarea contains two major shear zones: the interpreted SZ-II and the dextral KaSZ with south block up movement (Pitkälä 2019; Fig. 17a). In addition, subsidiary structures related to both shear zones were observed as well (Figs. 12c, 15e-g). The shear zones exhibit both brittle and ductile deformation fabrics. For example, brittle structures along and apparently splaying from the SZ-II that also exhibits ductile deformation fabrics indicate that a later deformation event took place in lower temperature conditions due to cooling of the crust and thus leading to faulting rather than shearing.

Some structures observed are spatially associated with the interpreted major shear zones and are apparently splaying from them (Fig. 17a). In addition, the western parts of southern subarea contain multiple NNW–SSE-trending shear bands (Fig. 17a). The larger subsidiary structures have mainly been formed under brittle regime (Figs. 12c, 15f, g) with one exception (Fig. 15e). Also, a roughly E–W trending brittle fault with dextral kinematics indicated by wing cracking which is possibly splaying from SZ-I was observed at locality 97 (Fig. 12c).

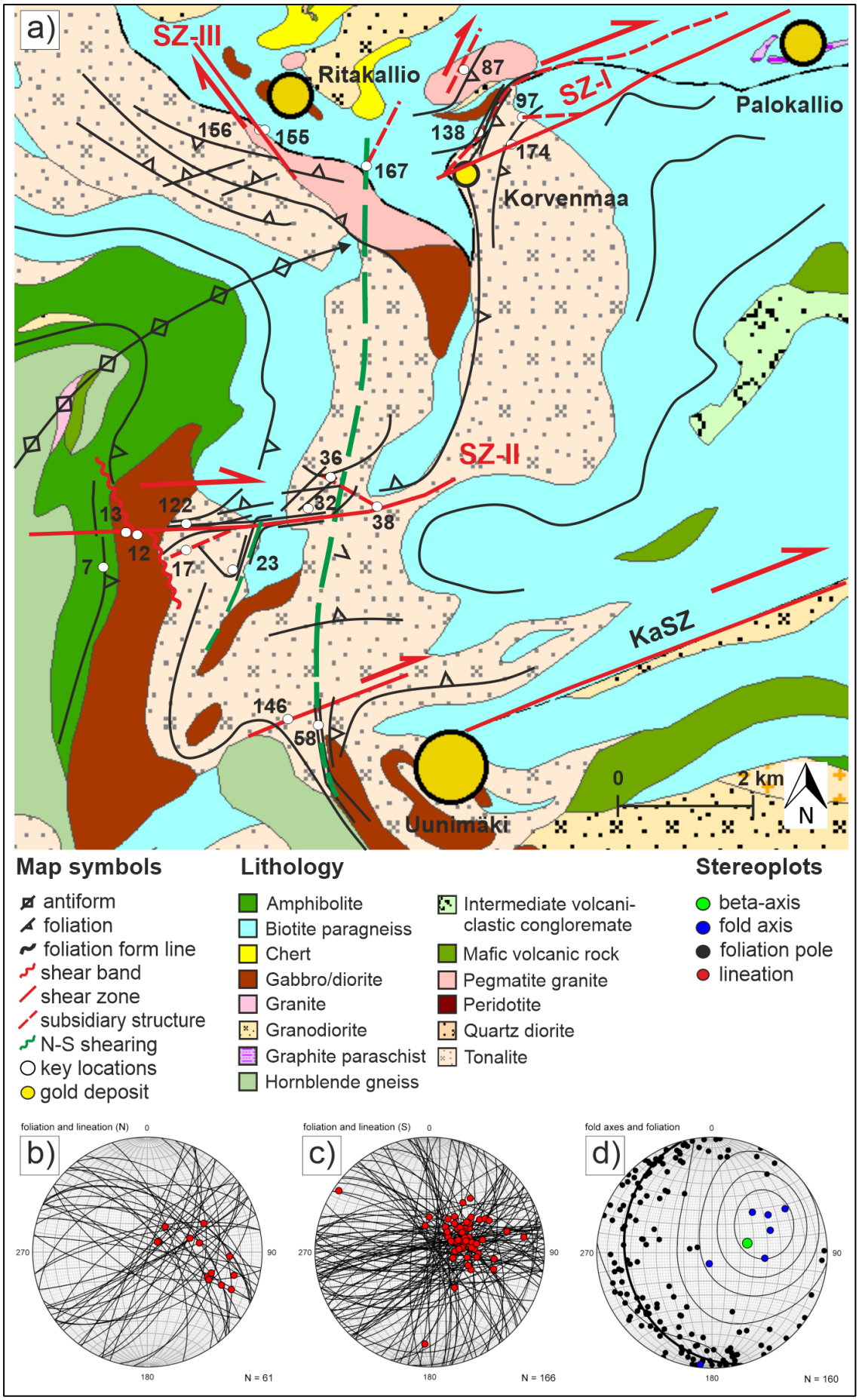

Figure 17. Caption overleaf.

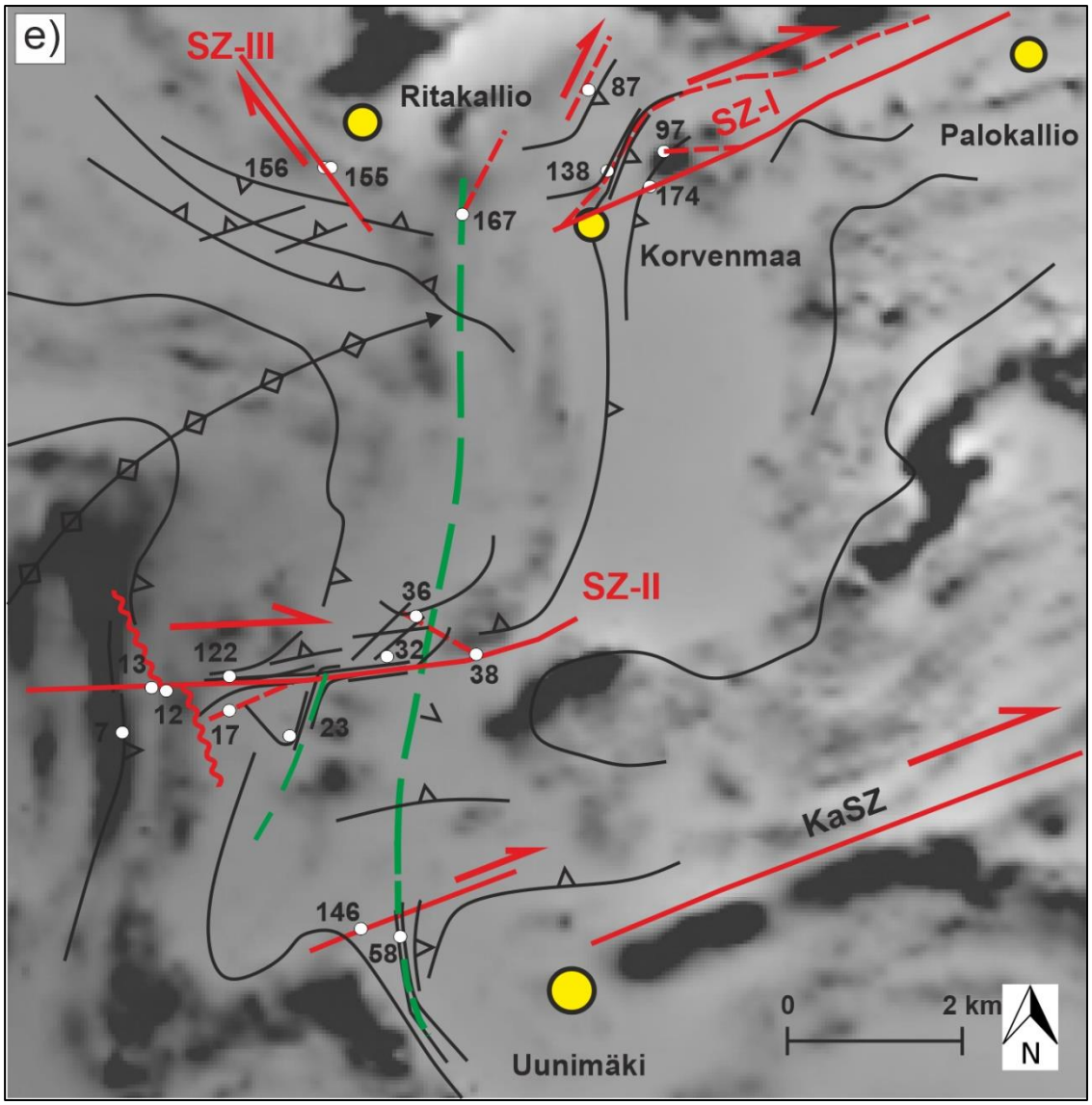

Figure 17. a) Structural map of the study area with subareas, form lines, major shear zones and known gold occurrences. Stereoplots illustrate foliation planes and mineral lineations in each subarea; b) northern and c) southern, and d) measured fold axes with foliation poles with best-fit-plane and β - axis from the whole study area. e) Structural map with aeromagnetic anomaly map in the background, Lithological and aeromagnetic background maps are provided by Geological Survey of Finland.

4.4 Pegmatites and veins

In total 33 felsic dikes, 31 quartz veins, and 25 pegmatites were measured in the whole study area. Stereographic projections reveal that the orientation distribution of foliation and dikes, pegmatites, and veins are similar (Fig. 18). In fact, the quartz veins and felsic dikes are commonly foliation parallel throughout the study area, but crosscutting ones are not uncommon either, occurring usually at an acute angle between 15–30° with respect to the foliation (Fig. 19c). The quartz veins observed in this study were commonly small with a thickness of 1–2 cm (Fig. 19c), whereas felsic dikes average thickness is ~5 cm (Fig. 13a). The biggest one found is located in the southern subarea, close to the western end of KaSZ, where a folded quartz vein within felsic volcanic unit was discovered (Fig. 19d). It must be

emphasized that pegmatites are more common than the numbers indicate as these were not of great interest in the field. The dominant host rock for dikes and veins is by far granodiorite. Although, this is not surprising as granodiorite is the most common rock type observed in this study.

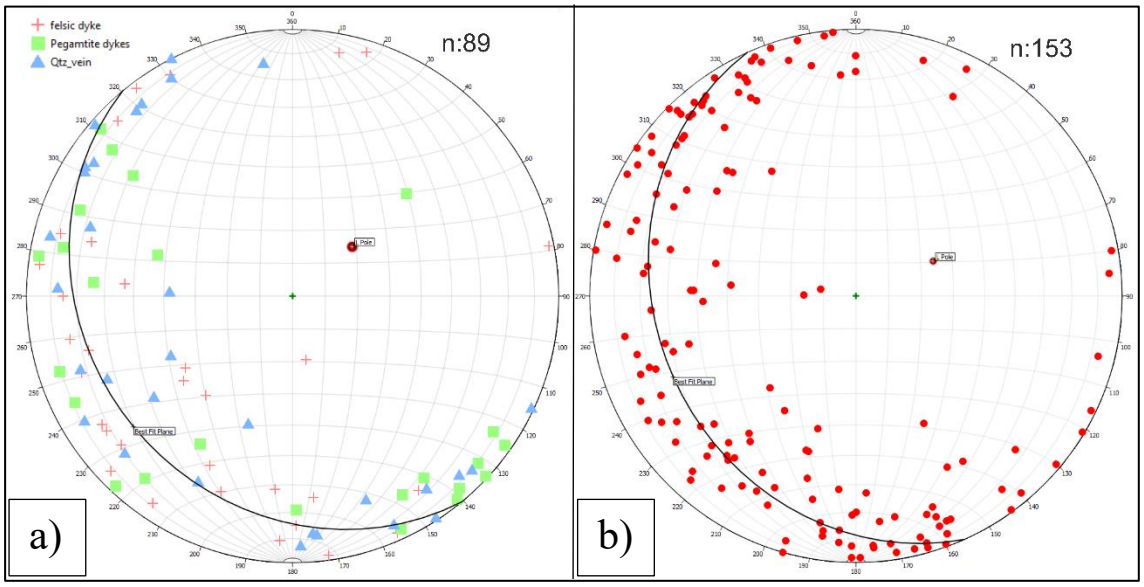

Figure 18. Stereographic projections of a) pole distribution of dikes and veins with best-fit-plane and L-pole (beta-axis/pole of best-fit-plane), b) foliation poles with best-fit-plane (beta-axis/pole of best-fit-plane).

The pegmatites in the study area can be classified into the deformed and undeformed pegmatites. Based on field observations the deformed pegmatites are more tonalitic in composition and slightly finer-grained than the sharply crosscutting undeformed pegmatites that are more granitic in composition. The crosscutting nature and the lack of mesoscopic deformation textures in the latter pegmatites indicate that they are post orogenic and probably related to an extensional phase in the area.

This said, the deformed pegmatites also exhibit crosscutting nature but have been folded together with the host rock (Fig. 19a). Also, the deformed pegmatites have undergone ductile boudinage as seen on few outcrops (Fig. 19b). These features indicate that they were already emplaced when ductile deformation took place. Altogether, it seems that the study area has undergone at least two extensional phases with contractional phase in between as the older pegmatites have undergone ductile deformation.

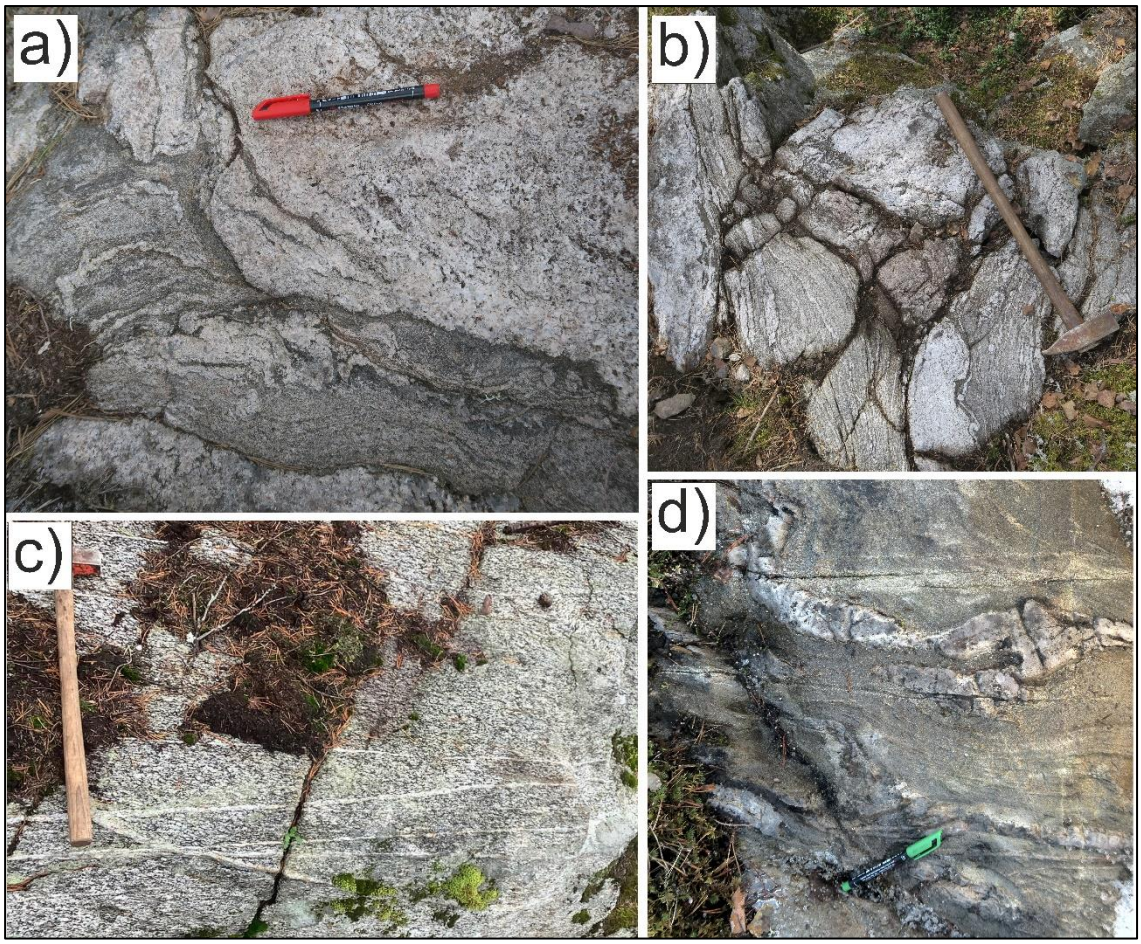

Figure 19. a) Pegmatite deformed together with surrounding mica gneiss, b) pegmatite exhibiting boudinage, c) typical foliation sub-parallel quartz-feldspar veins, d) folded quartz vein within felsic volcanic rock.

5 Discussion

The larger shear zones in the study area occur in three directions, i) ENE–WSW trending SZ-I and SZ-II, which are sub-parallel to parallel with the Kankaanranta SZ, ii) a (N)NW–(S)SE trending shear zone represented by SZ-III, and iii) a N–S trending shearing trailing through the central parts of the study area (Figs. 17a, 20). In addition, (N)NW–(S)SE trending shear structures such as shear bands and a shear zone (Figs. 15a, b) are common in western parts of the southern subarea, whereas (N)NE– (S)SW trending shear structures characterize the northern subarea (Figs. 12d, 16c, d). Also, the (N)NW–(S)SE trending shear structures in the southern subarea might be related to the ductile deformation that resulted in the regional folds (Fig. 20a).

The ENE–WSW trending SZ-I and SZ-II showcase dominantly dextral kinematics, but SZ-II also exhibits sinistral kinematics that can be explained by kinematic reversal of pre-existing shear zones taking place due to stress field reorientation in later deformation phases (e.g. Mattila & Viola 2014; Figs. 20b, c). Also, the orientation and kinematics of SZ-I are ambiguous, and it might comprise of several anastomosing branches of smaller shear zones indicated by the geophysical map (Figs. 9 & 17e). However, the brittle shear fractures at locality 97 that is spatially associated with the SZ-I indicate dextral kinematics and correspond well with early brittle stage 1 and subsequent stage 2 stress field at roughly 1.75 Ga (Mattila & Viola 2014). SZ-III is tentatively a dextral shear zone but remains ambiguous as well. In addition, the SZ-I and SZ-III interpreted here have been interpreted as part of a single shear zone that represents a continuum of the HSZ (GTK-MDAE 2022; Figs. 1 & 9).

The southern subarea expresses steep linear features plunging towards NE whereas northern subarea expresses a slightly more eastwards trending steep lineations (Figs. 17b, c). A large regional fold with axial plane that apparently curves slightly from NE trending towards E separates the subareas, hence the change in lineation plunge direction probably reflects that curved fold axial plane (Fig. 20a). In addition, SZ-I can be traced to the regional fold's axial plane, which is a potential weakness zone in bedrock (Fig. 20b).

The ENE–WSW trending shear zones SZ-I and SZ-II might represent regional ~E–W trending dominantly dextral shear zones associated with a continental collision that commenced at ~1.84 Ga (Väisänen & Skyttä 2007). This oblique collision event between Fennoscandia and Sarmatia took place under transpressive regime during the Svecobaltic orogeny at 1.84–1.80 Ga, which led to crustal shortening in ~N–S direction (Ehlers 1993; Lahtinen et al. 2005). After initial northward directed thrusting the bulk shortening direction

during this event was NW–SE in SW Finland (Väisänen & Skyttä 2007). Also, the KaSZ has been interpreted as a dextral oblique reverse fault with south side up kinematics resulting in crustal shortening under transpressive regime (Fig. 20d; Pitkälä 2019).

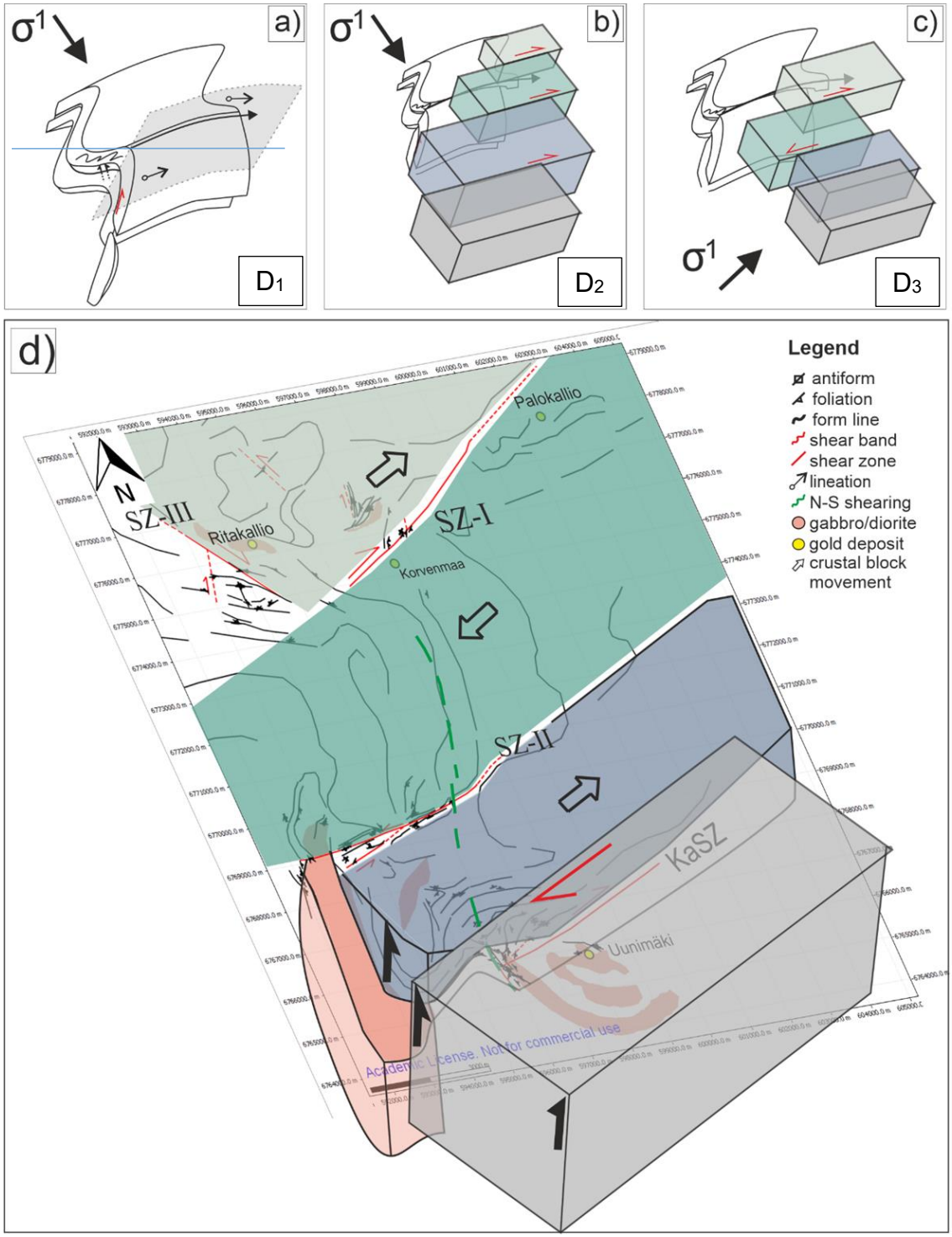

Figure 20. Schematic illustration of the tectonic evolution of the study area. a) Early deformation resulting in SW-NE oriented folding with curving axial plane leading to lineation plunging towards E in the northern subarea and to the NE in the southern subarea (blue line separates subareas). b) Late ductile deformation leading to ~E-W dextral shear zones with southside and westside up in the southern subarea. c) Switch in the orientation of the stress field leading to reactivation and reversal of previously formed shear zones under brittle regime. d) Schematic blocks in map view.

After the NW-SE oriented bulk shortening that formed regional folding in the study area, the strain started to partition leading to the formation of ~E-W trending dextral shear zones under retrograde phase, possibly crossing the brittle-ductile transition zone (D_2; Fig. 20b). For example, the NE–SW to WSW–ENE and NW–SE trending gold mineralization controlling structures in Satulinmäki and Riukka prospects formed during retrograde phase under brittle-ductile transitional setting (Saalmann 2007).

The contrasting shear senses between the shear zones SZ-I and SZ-II can be explained by westward movement of the block between these shear zones due to switch in the orientation of the stress field, which could create these kinematic indicators during later reactivation of the shear zones (Fig. 20c). Furthermore, the Jokisivu area exhibit faults with characteristics indicating a ~ NE–SW principal stress axis, which have been described as post-D_6 (D_3 this study; Fig. 20c) i.e., after Jokisivu gold mineralization (Fig. 20c; Saalmann et al. 2010). This indicates that the gold mineralization in the study area has taken place before D_3, most likely during D_2 (Fig. 20b).

The shift from the ductile late Svecofennian deformation and associated shear zones (1.81–1.79 Ga) to more brittle faulting and reactivation of earlier shear zones may be an important event as shifts in the stress field leading to a change in the tectonic regime from compressional to transpressional or transtensional, can trigger gold mineralization (Goldfarb & Groves 2015). For example, gold bearing quartz veins are associated with shear zones that formed under brittle–ductile transitional setting in a retrograde phase (Saalmann et al. 2009).

This said, the Korvenmaa and Palokallio gold occurrences are spatially associated with the tentative SZ-I, while the roughly NW–SE trending SZ-III is associated with Ritakallio gold occurrence that also hosts gold critical structures in this orientation along with roughly E–W trending ones (Vuori et al. 2005). Moreover, it has been proposed that the similarly ~E–W trending gold-hosting shear zones at Jokisivu splay from regional-scale NW–SE trending structures (Saalmann et al. 2010). The SZ-III might represent this major shear zone (Fig. 17a). Furthermore, NNE–SSW trending dextral shear bands were observed in the northern subarea. This trend has not been considered before as gold critical in the study area whereas the gold mineralizations in Kaapelinkulma deposit roughly 75 km to ENE are associated with narrow sinistral NNE–SSW trending shears that exhibit both ductile and brittle deformation (Rosenberg 1997).

This said, even with relatively small amount of field evidence of the shear zones interpreted in this thesis, the structural trends they exhibit may turn out to be important for future

exploration of orogenic gold in the study area. Especially, if subsidiary structures can be traced to suitable lithology such as gabbro or diorite that could act as traps for hydrothermal gold-bearing ore fluids, which are the dominant host rock for ore deposits in the study area (e.g. Eilu et al. 2012, and references therein). For example, the western end of SZ-II intersects northern part of a gabbro unit, in which ore hosting subsidiary structures may be present further south where the gabbro area continues (Fig. 17a). Also, NNE-SSW trending structures observed in the northern subarea may be gold critical (Fig. 17a).

5.1 Source of errors

It must be emphasized that SZ-I is tentative even though it is clearly visible in aeromagnetic anomaly map, but it was not identified in the field directly, whereas some indications of SZ-II were recognized in the field such as high strain rocks, shear bands, and faults (Fig. 13). SZ-III remains ambiguous as well, because more evidence from the field is required as clear indication of this shearing was observed in one outcrop only (Fig. 12d). Moreover, lithological observations are in some cases prone to errors as the weather conditions were rainy and muddy during some of the field workdays making it very difficult to obtain proper information.

6 Conclusions

- The gold occurrences within the study area are spatially associated with ENE–WSW and ~NW–SE trending shear zones.
- Regional folding exhibit fold axes that steeply plunge towards ~NE.
- The strain variation is not significant excluding the high strain zones, where the foliation is transposed into the orientation of adjacent shear zone.
- Pegmatites have been emplaced in two different phases.
- Older pegmatites have intruded and emplaced before ductile deformation has taken place whereas younger pegmatites crosscut sharply other rocks and lack of mesoscale deformation textures.
- The study area exhibits strong brittle overprinting on the ductile shear zones
- Changes in the stress field led to reactivation of earlier ductile shear zones in a brittle fashion during later deformation phases.

Acknowledgements

First, I would like to thank K.H. Renlund Foundation for funding this project. I would like to thank Professor Pietari Skyttä for managing this project and supervising this Thesis. Furthermore, his guidance during the field work and writing process is greatly appreciated. I would also like to thank Petroleum Experts Ltd (PETEX) for providing academic license to MOVE™ program.

References

Åhäll, K.-I. & Connelly, J. N. (2008). Long-term convergence along SW Fennoscandia: 330 m.y. of Proterozoic crustal growth. Precambrian Research, 163 (3-4), 402–421.

Anhaeusser, C.R. (1976). The nature and distribution of Archean gold mineralization of southern Africa. Minerals Science Engineering, 8, 46–84.

Arslan, A., Passchier, C. W., & Koehn, D. (2008). Foliation boudinage. Journal of Structural Geology, 30(3), 291–309.

Bierlein, F.P. & Crowe, D.E. (2000). Phanerozoic orogenic lode gold deposits. Reviews in Economic Geology, 13, 103–139.

Bingen, B., Andersson, J., Söderlund, U. & Möller, C. (2008). The Mesoproterozoic in the Nordic countries. Episodes 31, 29–34.

Bogdanova, S., Gorbatschev, R., Skridlaite, G., Soesoo, A., Taran, L. & Kurlovich, D. (2015). Trans–Baltic Palaeoproterozoic correlations towards the reconstruction of supercontinent Columbia/Nuna. Precambrian Research, 259, 5–33.

Bohlke, J.K. (1982). Orogenic (metamorphic-hosted) gold-quartz veins. U.S. Geological Survey, Open-file Report 795, 70–76.

Bowers, T.S. (1991). The deposition of gold and other metals: Pressure-induced fluid immiscibility and associated stable isotope signatures. Geochimica et Cosmochimica Acta, 55, 2417–2434.

Boyle, R.W. (1961). The geology, geochemistry, and origin of the gold deposits of the Yellowknife district. Canadian Geological Survey, Memoir 310. 193 p.

Cox, D.P. & Singer, D.A. (Eds.) 1986. Mineral Deposit Models. U.S. Geological Survey, Bulletin 1693. 379 p.

Daly, J. S., Balagansky, V. V., Timmermann, M. J., Whitehouse, M. J., de Jong, K., Guise, P., Bogdanova, S., Gorbatshev, R. & Bridgewater, D. (2001). Ion microprobe U–Pb zircon geochronology and isotopic evidence for a trans-crustal suture in the Lapland–Kola Orogen, northern Fennoscandian Shield. Precambrian Research, 105 (2–4), 289–314.

Daly, J. S., Balagansky, V. V., Timmermann, M.J. & Whitehouse, M. J. (2006). The Lapland–Kola orogen: Palaeoproterozoic collision and accretion of the northern Fennoscandian lithosphere. In: Gee, D.G. & Stephenson, R.A. (Eds.) European Lithosphere Dynamics. Geological Society, London, Memoirs 32, 579–598.

Ehlers, C., Lindroos, A. & Selonen, O. (1993). The late Svecofennian granite-migmatite zone of southern Finland – a belt of transpressive deformation and granite emplacement. Precambrian Research, 64, 295–309.

Eilu, P. (2012). Gold mineralisation in southwestern Finland. Geological Survey of Finland, Special Paper 52, 11–22.

Eilu, P. (2015). Overview on Gold Deposits in Finland. Mineral Deposits of Finland, 377–410.

Eilu, P. & Pankka, H. (2010). FINGOLD – A public database on gold deposits in Finland. Version 1.1. Geological Survey of Finland. Digitaalisest tietotuotteet 10. Optical disc (CD-ROM). Available at: https://tupa.gtk.fi/julkaisu/digitaalinentuote/fingold.zip

Eilu, P., Sorjonen-Ward, P., Nurmi, P. & Niiranen, T. (2003). A Review of Gold Mineralization Styles in Finland. Economic Geology, 98, 1329–1353.

Eisenlohr, B.N., Groves, D.I. & Partington, G.A. (1989). Crustal-scale shear zones and their significance to Archean gold mineralization in Western Australia. Mineralium Deposita, 24, 1–8.

Fedorowich, J., Stauffer, M. & Kerrich, R. (1991). Structural setting and fluid characteristics of the Proterozoic Tartan Lake gold deposit, Trans–Hudson orogen, northern Manitoba. Economic Geology, 92, 552–568.

Frimmel, H. E. (2008). Earth's continental crustal gold endowment. Earth and Planetary Science Letters, 267(1–2), 45–55.

Fryer, B.J., Kerrich, R., Hutchinson, R.W., Peirce, M.G. & Rogers, D.S. (1979). Archean precious-metal hydrothermal systems, Dome Mine, Abitibi greenstone belt. I. Patterns of alteration and metal distribution. Canadian Journal of Earth Sciences, 16, 421–439.

Gaál, G. & Gorbatschev, R. (1987). An outline of the Precambrian evolution of the Baltic Shield. Precambrian Research, 35, 15–52.

Gebre-Mariam, M., Hagemann, S.G., Groves, D.I., (1995). A classification scheme for epigenetic Archaean lode-gold deposits. Mineralium Deposita, 30, 408–410.

Goldfarb, R.J. & Groves, D.I. (2015). Orogenic gold: Common or evolving fluid and metal sources through time. Lithos, 233, 2–26.

Goldfarb, R.J., Groves, D.I. & Gardoll, S. (2001). Orogenic gold and geologic time: a global synthesis. Ore Geology Reviews, 18, 1–75.

Goldfarb, R.J., Baker, T., Dubé, B., Groves, D.I., Hart, C.J.R., Gosselin, P., (2005). Distribution, character, and genesis of gold deposits in metamorphic terranes. Economic Geology 100th Anniversary, 407–450.

Goldfarb, R. J., Bradley, D., & Leach, D. L. (2010). Secular variation in economic geology. Economic Geology, 105(3), 459–465.

Gorbatschev, R. & Bogdanova, S. (1993). Frontiers in the Baltic Shield. Precambrian Research, 64, 3–21.

Grasemann, B., Martel, S., & Passchier, C. (2005). Reverse and normal drag along a fault. Journal of Structural Geology, 27(6), 999–1010.

Groves, D.I. & Phillips, G.N. (1987). The genesis and tectonic control on Archaean gold deposits of the Western Australian Shield – A metamorphic replacement model. Ore Geology Reviews, 2, 287–322.

Groves, D.I., Goldfarb, R.J., Gebre-Mariam, M., Hagemann, S.G. & Robert, F. (1998). Orogenic gold deposits: a proposed classification in the context of their crustal distribution and relationship to other gold deposit types. Ore Geology Reviews, 13, 7–27.

Groves, D.I., Goldfarb, R.J., Robert, F. & Hart, C.J.R. (2003). Gold deposits in metamorphic belts: overview of current understanding, outstanding problems, future research, and exploration significance. Economic Geology, 90, 1–30.

Groves, D.I., Ridley, J.R., Bloem, E.M.J., Gebre-Mariam, M., Hagemann, S.G., Hronsky, J.M.A., Knight, J.T., McNaughton, N.J., Ojala, J., Vieheicher, R.M., McCuaig, T.C. & Holyland, P.W. (1995). Lode gold deposits of the Yilgam Block: products of late-Archean crustal-scale overpressured hydrothermal systems. Ire Coward, M.P. & Ries, A.C. (Eds.), Early Precambrian Processes. Geological Society of London, Special Publications, 95, 155–172.

Groves, D.I., Santosh, M. & Deng, J. (2020). A holistic model for the origin of orogenic gold deposits and its implications for exploration. Mineralium Deposita, 55, 275–292.

Grönholm, S. & Voipio, T. (2012). The Palokallio gold occurrence at Huittinen, southern Finland. Geological Survey of Finland, Special Paper 52, 91–99.

GTK. (2020). Overview of the Orogenic Gold Metallogeny in Finland. <https://minsysfin.gtk.fi/index.php/overview-of-the-orogenic-gold-metallogeny-in-finland/>, acquired 18.4.2022.

GTK-MDAE (2022). Mineral Deposits and Exploration. <gtkdata.gtk.fi/mdae/index.html>, acquired 15.10.2022.

Hanski, E. & Huhma, H. (2005). Central Lapland greenstone belt. In: Lehtinen, M., Nurmi, P. & Rämö, T. (Eds.) The Precambrian Bedrock of Finland—Key to the Evolution of the Fennoscandian Shield. Elsevier, Amsterdam, 139–194.

Hayashi, K. & Ohmoto, H. (1991). Solubility of gold in NaCl and H_2S-bearing aqueous solutions at 250–350°C. Geochimica et Cosmochimica Acta, 55, 2111–2126

Hermansson, T., Stephens, M.B., Corfu, F., Page, L.M., Andersson, J., (2008). Migratory tectonic switching, western Svecofennian orogen, central Sweden: Constraints from U/Pb zircon titanite geochronology. Precambrian Research, 161, 250–278.

Holden, E. J., Wong, J. C., Kovesi, P., Wedge, D., Dentith, M., & Bagas, L. (2012). Identifying structural complexity in aeromagnetic data: An image analysis approach to greenfields gold exploration. Ore Geology Reviews, 46, 47–59.

Hronsky, J.M.A., Cassidy, K.F., Grigson, M.W., Groves, D.I., Hagemann, S.G., Mueller, A.G., Ridley, J.R., Skwarnecki, M.S. & Vearncombe, J.R. (1990). Deposit- and mine-scale structure. In: Ho, S.E., Groves, D.I. & Bennett, J.M. (Eds.), Gold deposits of the Archean Yilgarn Block, Western Australia: Nature, Genesis and Exploration Guides. Nedlands, W.A: Geology Key Centre & University Extension, University of Western Australia, Publication 20, 38–59

Hubbard, F., & Branigan, N. (1987). Late svecofennian magmatism and tectonism, Åland, Southwest Finland. Precambrian Research, 35, 241–256.

Hudleston, P. J. (1989). The association of folds and veins in shear zones. Journal of Structural Geology, 11(8), 949–957.

Hölttä, P., Balagansky, V., Garde, A.A., Mertanen, S., Peltonen, P., Slabunov, A., Sorjonen-Ward, P. & Whitehouse, M. (2008). Archean of Greenland and Fennoscandia. Episodes 31, 1–7.

Hölttä, P., Heilimo, E., Huhma, H., Kontinen, A., Mertanen, S., Mikkola, P., Paavola, J., Peltonen, P., Semprich, J., Slabunov, A. & Sorjonen-Ward, P. (2012). The Archaean of the Karelia Province in Finland. In: Hölttä, P. (Ed.) The Archaean of the Karelia Province in Finland. Geological Survey of Finland, Special Paper 54, 21–73.

Jurvanen, T., Eklund, O., & Väisänen, M. (2005). Generation of A-type granitic melts during the late Svecofennian metamorphism in southern Finland. GFF, 127(2), 139–147.

Kara, J., Leskelä, T., Väisänen, M., Skyttä, P., Lahaye, Y., Tiainen, M., & Leväniemi, H. (2021). Early Svecofennian rift-related magmatism: Geochemistry, U-Pb-Hf zircon isotope data and tectonic setting of the Au-hosting Uunimäki gabbro, SW Finland. Precambrian Research, 364, 106364.

Kerrich, R. (1989a). Geochernical evidence on the sources of fluids and solutes for shear zone hosted mesothermal Au deposits. In: Bursnall, J.T. (Ed.), Mineralization and Shear Zones. Geological Association of Canada Short Course Notes 6, 129–197.

Kerrich, R. (1989b). Source processes for Archean Au-Ag vein deposits; evidence for lithophile-element systematics of the Hollinger-McIntyre and Buffalo Ankerite deposits, Timmins. Canadian Journal of Earth Sciences, 26, 755–781.

Kerrich, R. (1989c). Archean gold—relationship to granulite formation or felsic intrusions? Geology, 17, 1011–1015.

Kerrich, R. (1993). Perspectives on genetic models for lode-gold deposits. Mineralium Deposita, 28, 362–365.

Kilpeläinen, T. (1998). Evolution and 3D modelling of structural and metamorphic patterns of the Palaeoproterozoic crust in the Tampere-Vammala area, southern Finland. Geological Survey of Finland, Bulletin 397. 124 p.

Korja, A., Lahtinen, R., & Nironen, M. (2006). The Svecofennian orogen: a collage of microcontinents and island arcs. Geological Society, London, Memoirs, 32(1), 561–578.

Korsman, K., Koistinen, T., Kohonen, J., Wennerström, M., Ekdahl, E., Honkamo, M., Idman, H. & Pekkala, Y. (Eds.) 1997. Suomen kallioperäkartta – Berggrundskarta över Finland – Bedrock map of Finland 1:1 000 000. Geological Survey of Finland.

Korsman, K., Korja, T., Pajunen, M., Virransalo, P. & GGT/SVEKA Working Group (1999). The GGT/SVEKA Transect: structure and evolution of the continental crust in the Palaeoproterozoic Svecofennian orogen in Finland, International Geology Review, 41 (4), 287–333.

Kärkkäinen, N. (2007). HANKE 2901003. Etelä- ja Länsi-Suomen kultavarojen kartoitus. Loppuraportti toiminnasta 2002–2007. Geological Survey of Finland, report M10.4/2007/10/71.

Kärkkäinen, N., Huhta, P., Lehto, T., Tiainen, M., Vuori, S. & Pelkkala, M. (2012). New geochemical data for gold exploration in southern Finland. Geological Survey of Finland, Special Paper 52, 23–46,

Kärkkäinen, N., Koistinen, E., Huotari-Halkosaari, T., Kuusela, J., Muhammad, S. & Huhta, P. (2016). Uunimäki gold deposit at Huittinen, Southwest Finland. Geological Survey of Finland, Archive Report 77, 54 p.

Lahtinen, R. (1994). Crustal evolution of the Svecofennian and Karelian domains during 2.1 – 1.79 Ga, with special emphasis on the geochemistry and origin of 1.93–1.91 Ga gneissic tonalities and associated supracrustal rocks in the Rautalampi area, central Finland. Geological Survey of Finland, Bulletin 378. 128 p.

Lahtinen, R. (1996). Geochemistry of Palaeoproterozoic supracrustal and plutonic rocks in the Tampere-Hämeenlinna area, southern Finland. Geological Survey of Finland, Bulletin 389. 113 p.

Lahtinen, R., Korja, A. & Nironen, M. (2005). Paleoproterozoic tectonic evolution. In: Lehtinen, M., Nurmi, P.A. & Rämö, O.T. (Eds.), Precambrian Geology of Finland – Key to the Evolution of the Fennoscandian Shield. Elsevier B.V., Amsterdam, 481–532.

Lahtinen, R., Korja, A., Nironen, M., & Heikkinen, P. (2009). Palaeoproterozoic accretionary processes in Fennoscandia. Geological Society, London, Special Publications, 318(1), 237–256.

Lahtinen, R., Huhma, H., Lahaye, Y., Kousa, J. & Luukas, J. (2015). Archean–Proterozoic collision boundary in central Fennoscandia: Revisited. Precambrian Research, 261, 127–165.

Leskelä, T. (2019). Geochemistry, age and structural character of the Au-hosting Uunimäki gabbro, SW Finland, 84 p.

Lindgren, W. (1933). Mineral Deposits. 4th ed. McGraw Hill, New York and London. 930 p.

Luukkonen, A., Grönholm, P. & Hannila, T. (1992). Eräiden Etelä-Suomen kulta- ja sen seuralaismetalliesiintymien geologiset pääpiirteet. Summary: Main geological features of certain gold and tungsten-tin-gold prospects in Southern Finland. Geologian tutkimuskeskus 113, 90 p.

Luukkonen, A. (1994). Main geochemical features, metallogeny and hydrothermal alteration phenomena of certain gold and gold-tin-tungsten prospects in southern Finland. Geological Survey of Finland, Bulletin 377. 153 p.

Mattila, J. & Viola, G. (2014). New constraints on 1.7 Gyr of brittle tectonic evolution in southwestern Finland derived from a structural study at the site of a potential nuclear waste repository (Olkiluoto Island). Journal of Structural Geology, 67, 50–74.

McCuaig, T. C. & Kerrich, R. (1998). P—T—t—deformation—fluid characteristics of lode gold deposits: evidence from alteration systematics. Ore Geology Reviews, 12, 381–453.

Mikucki, E. J. (1998). Hydrothermal transport and depositional processes in Archean lode-gold systems: A review. Ore Geology Reviews, 13(1–5), 307–321.

Molnár, F., O'Brien, H., Stein, H., & Cook, N. D. (2017a). Geochronology of hydrothermal processes leading to the formation of the Au–U mineralization at the Rompas prospect, Peräpohja belt, Northern Finland: Application of paired U–Pb dating of

uraninite and Re–Os dating of molybdenite to the identification of multiple hydrothermal events in a metamorphic terrane. Minerals, 7(9), 171.

Molnár, F., O´Brien, H., Lahaye, Y., Kurhila, M., Middleton A. & Johanson, B. (2017b). Multi-stage hydrothermal processes and diverse metal associations in orogenic gold deposits of the Central Lapland Greenstone Belt, Finland. Mineral Resources to Discover – 14th SGA Biennial Meeting 2017, Volume 1, 63–66.

Mouri, H., Korsman, K., & Huhma, H. (1999). Tectono-metamorphic evolution and timing of the melting processes in the Svecofennian Tonalite-Trondhjemite Migmatite Belt: an example from Luopioinen, Tampere area, southern Finland. Bulletin of the Geological Society of Finland, 71(1), 31-56.

Mäkelä, K. (1980). Geochemistry and origin of Haveri and Kiipu, Proterozoic strata bound volcanogenic gold copper and zinc mineralizations from southwestern Finland. Geological Survey of Finland, Bulletin 310. 79 p.

Nironen, M. (1989). The Tampere schist belt: Structural style within an early Proterozoic volcanic arc system in southern Finland. Precambrian Research, 43, 23–40.

Nironen, M. (1994). Structural control and (re)mobilization of the extinct Haveri Au-Cu deposit, southern Finland. Bulletin of the Geological Society of Finland, 66, 39–44.

Nironen, M. (2017). Guide to the Geological Map of Finland – Bedrock 1:1 000 000. Geological Survey of Finland, Special Paper 60, 41–76.

Nordbäck, N., Mattila, J., Zwingmann, H. & Viola, G. (2022). Precambrian fault reactivation revealed by structural and K-Ar geochronological data from the spent nuclear fuel repository in Olkiluoto, southwestern Finland. Tectonophysics, 824, 229208.

Ojala, V. J. (2003). Satulinmäki Au prospect structural mapping. Geological Survey of Finland, unpublished report CM19/2024/2003/1/10. 13 p.

Peltonen, P., & Kontinen, A. (2004). The Jormua ophiolite: A mafic-ultramafic complex from an ancient ocean-continent transition zone. Developments in Precambrian Geology, 13, 35–71.

Peters, S.G. (1993a). Nomenclature, concepts and classification of oreshoot in vein deposits. Ore Geology Reviews, 8, 3–22.

Peters, S.G. (1993b). Formation of oreshoots in mesothermal gold-quartz vein deposits: examples from Queensland, Australia. Ore Geology Reviews, 8, 277–301.

Phillips, G.N. & Evans, K.A. (2004). Role of CO2 in the formation of gold deposits. Nature 429, 860–863.

Phillips, G.N. & Powell, R. (1993). Link between gold provinces. Economic Geology, 88, 1084–1098.

Phillips, G. N. & Powell, R. (2015). A practical classification of gold deposits, with a theoretical basis. Ore Geology Reviews, 65, 568–573.

Pitkälä, I. (2019). Shear zones and structural analysis of the Loimaa area, SW Finland, 72 p.

Poulsen, K.H. (1996). Lode-gold. In: Eckstrand, O.R., Sinclair, W.D., Thorpe, R.I. (Eds.), Geology of Canadian Mineral Deposit Types. The Geology of North America, vol. P-1. Geological Society of America, 323–328.

Poulsen, K.H., Robert, F., Dube, B., (2000). Geological classification of Canadian gold deposits. Geological Survey of Canada Bulletin 540, 106 p.

Puustinen, K. (1991). Gold deposits of Finland: Journal of Geochemical Exploration, 39, 255–272.

Puustinen, K. (2003). Suomen kaivosteollisuus ja mineraalisten raaka-aineiden tuotanto vuosina 1530–2001, historiallinen katsaus erityisesti tuotantolukujen valossa. Geological Survey of Finland, Report M10.1/2003/3. 578 p.

Ranta, J. P., Molnár, F., Hanski, E., & Cook, N. (2018). Epigenetic gold occurrence in a Paleoproterozoic meta-evaporitic sequence in the Rompas-Rajapalot Au system, Peräpohja belt, northern Finland. Bulletin of the Geological Society of Finland, 90(1).

Reimers, S., Engström, J. & Riller, U. (2018). The Kynsikangas shear zone, Southwest Finland: Importance for understanding deformation kinematics and rheology of lower crustal shear zones. Lithosphere 2018 Symposium, November 14–16, 2018, Oulu, Finland, 95–97.

Ridley, J.R. (1993). The relations between mean rock stress and fluid flow in the cmst, with reference to vein- and lode-style gold deposits. Ore Geology Reviews, 8, 23–37.

Robb, L. (2005). Introduction to ore-forming processes. Blackwell Publishing Ltd. Oxford. 345 p.

Robert, F., Sheahan, P.A. & Green, S.B. (Eds.) 1991. Greenstone Gold and Crustal Evolution. Geological Association of Canada. Mineral Deposits Division Publication. 252 p.

Rosenberg, P. (1997). The Kaapelinkulma gold deposit, Valkeakoski. In: Ehlers, C. (Ed.) Gold and base metal deposits in southwestern Finland. Geological Survey of Finland, Guide 44, 23−25.

Rämö, O. T. & Haapala, I. (2005). Rapakivi granites. In: Lehtinen, M., Nurmi, P.A. & Rämö, O.T. (Eds.) Precambrian Geology of Finland – Key to the Evolution of the Fennoscandian Shield. Elsevier B.V., Amsterdam, 533–562.

Saalmann, K. (2007). Structural control on gold mineralization in the Satulinmäki and Riukka prospects, Häme Schist Belt, southern Finland. Bulletin of the Geological Society of Finland, 79, 69–93.

Saalmann, K., Mänttäri, I., Ruffet, G. & Whitehouse, M.J. (2009). Age and tectonic framework of structurally controlled Palaeoproterozoic gold mineralization in the Häme belt of southern Finland. Precambrian Research, 174, 53–77.

Saalmann, K., Mänttäri, I., Peltonen,P., Whitehouse, M.J., Grönholm, P. & Talikka, M. (2010). Geochronology and structural relationships of mesothermal gold mineralization in the Palaeoproterozoic Jokisivu prospect, southern Finland. Geological Magazine, 147, 551–569.

Shelton, K.L., So, C.-S., & Chang, J.S. (1988). Gold-rich mesothermal vein deposits of the Republic of Korea: geochemical studies of the Jungwon gold area. Economic Geology, 83, 1221–1237.

Sibson, R.H., & Scott, J. (1998). Stress / fault controls on the containment and release of overpressured fluids: Examples from gold-quartz vein systems in Juneau, Alaska; Victoria, Australia and Otago, New Zealand. Ore Geology Reviews, 13, 293–306.

Stefansson, A., & Seward, T.M. (2004). Gold(I) complexing in aqueous sulphide solutions to 500°C at 500 bar. Geochimica et Cosmochimica Acta, 68, 4121–4143.

Stuwe, K., Will, T.M. & Zhou, S. (1993). On the timing relationship between fluid production and metamorphism in metamorphic piles: Some implications for the origin of post-metamorphic gold mineralization. Earth and Planetary Science Letters, 114, 417–430.

Sundblad, K. (2003). Metallogeny of gold in the Precambrian of northern Europe. Economic Geology, 98, 1271–1290.

Tavares Nassif, M., Monecke, T., Reynolds, T. J., Kuiper, Y. D., Goldfarb, R. J., Piazolo, S., & Lowers, H. A. (2022). Formation of orogenic gold deposits by progressive movement of a fault-fracture mesh through the upper crustal brittle-ductile transition zone. Scientific Reports, 12(1), 1–11.

Tiainen, M., Kujala, S., Ahtola, T., Eilu, P., Grönholm, S., Hakala, O., Istolahti, P., Jumppanen, A., Kärkkäinen, N., Rasilainen, K., Törmä, H. (2017). Summary: Regional economic impacts of potential mining in Kanta-Häme. Geological Survey of Finland, research report, 229. 126 p.

Vaasjoki, M. & Huhma, H. (1999). Lead and neodymium isotopic results from metabasalts of the Haveri Formation, southern Finland: evidence for Palaeoproterozoic enriched mantle. Bulletin of the Geological Society of Finland, 71, 143–153.

Vuori, S. Kärkkäinen, N., Huhta, P. & Valjus, T. (2005). Ritakallio gold prospect, Huittinen, SW Finland. Geological Survey of Finland, unpublished report CM06/2112/2005/1/10. 53 p.

Väisänen, M. & Skyttä, P. (2007). Late Svecofennian shear zones in southwestern Finland. GFF, 129, 55–64.